Title

Molecular glues for protein-protein interactions: Progressing toward a new dream

Authors

Konstantinidou, Markella
Arkin, Michelle R

Publication Date

2024-05-01

DOI

10.1016/j.chembiol.2024.04.002

Molecular glues for protein-protein interactions: progressing towards a new dream

Markella Konstantinidou[1] and Michelle R. Arkin[1]*

[1]Department of Pharmaceutical Chemistry and Small Molecule Discovery Center (SMDC), University of California, San Francisco 94143, United States
Correspondence: michelle.arkin@ucsf.edu

Summary
The modulation of protein-protein interactions with small molecules is one of the most rapidly developing areas in drug discovery. In this review, we discuss advances over the past decade (2014-2023) focusing on molecular glues (MG) – monovalent small molecules that induce proximity, either by stabilizing native interactions or by inducing neomorphic interactions. We include both serendipitous and rational discoveries and describe the different approaches that were used to identify them. We classify the compounds in three main categories: degradative MGs, non-degradative MGs or PPI stabilizers, and MGs that induce self-association. Diverse, illustrative examples with structural data are described in detail, emphasizing the elements of molecular recognition and cooperative binding at the interface that are fundamental for a molecular-glue mechanism of action.

Keywords molecular glues, degraders, covalent, stabilizers, molecular recognition, PPI, ternary complex, cooperativity, proximity, native interactions, neomorphic

Introduction

Protein-protein interaction (PPI) networks play a central role in biological processes, including cell signaling, homeostasis, cell proliferation and differentiation. They are often dysregulated in diseases and thus have become a significant focus of chemical biology and drug discovery. In our previous decennial reviews we described PPI inhibitors, discussing the unique properties and challenges associated with the discovery of PPI inhibitors in 2004[1] and then their evolution towards clinical trials in 2014.[2] In the last ten years, the field of PPI modulation has rapidly evolved and expanded to new, fascinating directions. In our current review, we shift our focus from PPI inhibition to molecular glues and PPI stabilization, covering the period between 2014-2023. We are particularly interested in this new direction because stabilizing – rather than inhibiting – PPIs has the potential to target intrinsically disordered proteins (IDPs). Many IDPs remain important "undruggable" targets. However, upon binding to their protein partners, disordered domains may form ordered and ligandable structures at the PPI interface. Furthermore, targeting a protein pair allows modulation of a single complex for a scaffolding protein that interacts with many partners.

Many terms have appeared recently to describe these emerging concepts, including "chemically induced proximity", "molecular glues", "molecular glue degraders" and "PPI stabilizers". Quite often these terms are used interchangeably, despite underlying differences in these modalities. Herein we consider "molecular glues" (MGs) as monovalent small molecules that bind cooperatively at a PPI interface. Typically, MGs have low or unmeasurable affinity to at least one of the protein partners; upon binding, they enhance or strengthen interactions at the interface. MGs can bind either to native or non-native / neomorphic PPIs. The term "molecular glue degraders" (MGDs) refers to the subclassification of MGs in

which the binding partner is an E3 ubiquitin ligase (E3 ligase). E3 ligases transfer ubiquitin onto a substrate protein, usually to target that protein for degradation through the proteasome. MGDs induce native or non-native proteins-of-interest to be ubiquitinated by the E3 and lead to the proteins' proteasomal degradation. "PPI stabilizers", another subtype of MGs, usually refers to two protein partners that have intrinsic affinity in the absence of the glue, indicating native PPIs as the target. Here, we distinguish PPI stabilizers from allosteric stabilizers of a single protein. One more subtype of MGs includes compounds that induce self-association with or without degradation of the target as the outcome. In this case, binding of MGs results in high-order protein assemblies, usually in unexpected ways. The formed (ternary) complex differs significantly from the native state of the protein target. No specific term is used in the literature to describe these MGs, though occasionally the term "target aggregation" appears. In our point of view "target aggregation" is associated with the formation of energetically stable protein assemblies in which misfolded or misassembled proteins aggregate, often associated with a disease phenotype rather than a state that is compound-induced. Finally, the term "induced-proximity" is broader, and although in some cases appropriate for MGs, it also includes allosteric effects that do not necessarily fall under the glue-type mechanism of action.

In the last 10 years, numerous examples of MGs have been identified. Their discoveries have varied from serendipitous discoveries where the mechanism of action remained elusive, to more recent examples of rationally designed MGs. Here, we review examples from the three main types of molecular glues: degradative MGs, non-degradative MGs or PPI stabilizers, and MGs that induce self-association. It must be noted, however, that due to the diversity and complexity of MGs, some examples might belong in more than one category. The supplementary table (table S1) includes an overview of the MGs described here, their classification and the main experimental techniques used to establish the molecular-glue type of action. We emphasize the common features of MGs, namely, the elements of molecular recognition and cooperative binding at the interface. The goal here is not to provide an exhaustive catalog of known MGs, but instead to describe distinct examples with structural information and to show the vastly differently approaches that have led to their discovery. Many excellent reviews have been published recently covering chemically induced proximity modalities, including molecular glues.[3–6]

Molecular glues, as monovalent modalities, are typically low molecular weight compounds, with the exception of some natural products, and have favorable properties for further clinical development. Because the PPI interface targeted by MGs is "structured," the individual proteins do not necessarily need to contain well-defined binding pockets. Thus, targets once considered "undruggable" or "unligandable," such as transcription factors and intrinsically disordered proteins (IDPs), are now within reach for molecular glues. All subtypes of molecular glues, targeting native or neomorphic PPIs with degradative or non-degradative outcomes rely on molecular recognition and lead to the cooperative binding at an interface. As shown in the examples described here, quite often the solvent-exposed moiety of the glue is responsible for initiating its mechanism of action. For certain molecular glue degraders, degrons (on the client protein/neosubstrate) and hotspot gluing residues (on the ligase) are now defined, allowing the rational optimization or redirection of MGDs. In other cases, the precise molecular recognition features are not yet fully elucidated.

Directly related to discovery of the first MGDs, and in parallel to the development of monovalent MGs, the field of heterobifunctional modalities has also rapidly evolved. After the invention of proteolysis-targeting chimeras (PROTACs),[7] heterobifunctional molecules that rely on the recruitment of an E3 ligase to degrade the protein of interest (POI), a diverse array of new proximity-based modalities followed. Their applications cover a large set of post-translational modifications and mechanisms of degradation. These modalities have been extensively reviewed elsewhere, and are mechanistically distinct in several respects.[8–10] Bivalent molecules such as PROTACs include two ligands that bind – often with high affinity – to the individual proteins, connected by a linker that might play a role in formation of the ternary complex.[11] One of the exciting features of MGDs and bifunctional molecules is their "event-driven pharmacology."[10,12] Classic inhibitors directly block the function of the target protein and thus display occupancy-driven pharmacology. By contrast, the new modalities, especially those with a degradative outcome, eliminate the target protein and result in a superior and sustained pharmacological effect. For MGDs and PROTACs, the target elimination reduces both the enzymatic and scaffolding functions of the target proteins.[10,12]

For both modalities (monovalent molecular glues and heterobifunctional PROTACs) the term "cooperativity" is used to quantify a key feature. The structural differences between the two modalities lead to a differentiation of the meaning of cooperativity. For PROTACs, cooperativity (α) refers to the ratio of binary binding affinity (ligase/PROTAC; K_{LP}) to ternary binding affinity (ligase/PROTAC/target; K_{LPT}). Thus, cooperativity describes the effect of a binding partner (such as the E3 ligase) on the PROTAC's interaction with the other binding partner (POI). The outcome can be synergistic ($\alpha>1$), antagonistic ($\alpha<1$) or non-cooperative ($\alpha=1$).[11,13]It is noteworthy that some PROTACs demonstrate target degradation even in the absence of positive cooperativity.[14–16] On the contrary, for MGs the term cooperativity quantifies the effect of glue binding on the PPI. In other words, it refers to the ratio of Kd of the binary (Kd^{binary}) versus ternary PPI complex ($Kd^{ternary}$), in the absence versus presence of the glue. Thus, cooperativity is a defining feature for MGs, especially for the formation of neomorphic interactions, where there is low/no affinity for at least one of the binding partners. An additional difference between the two modalities is the hook effect that is often encountered for bifunctional molecules, since the compounds can bind to one protein individually and thus, at high concentrations, suppress formation of the ternary complex. On the other hand, typical MGs do not cause a hook effect because they show measurable binding affinity to (at most) one protein in the complex and induce cooperative association.

Degradative Molecular Glues

Natural products

Several classes of natural products acting as molecular glue degraders have been identified retrospectively. In 2001, Gray *et al.*[17] showed that the plant hormone auxin promoted the degradation of the transcription repressors AUX/IAA. In 2007, Tan *et al*.[18] provided the structural basis for auxin's mechanism of action. Crystal structures revealed that auxin enhanced weak interactions formed between AUX/IAA and TIR1, which is part of the E3 ligase complex SCF^{TIR1}, by binding to the beta propeller domain of TIR1 below the AUX/IAA binding site. In 2010, Sheard *et al.*[19] showed that the plant hormone methyl jasmonate acted via

a similar mechanism and degraded the transcriptional repressor JAZ by recruiting the E3 ligase SCF^{COI1}. These early examples showed the ability of small molecules to induce proximity to an E3 ubiquitin ligase and degrade the binding partner. They also inspired further studies for the identification of natural degradative glues. For example, in 2020, streptomyces-derived manumycin polyketides (manumycin A and asukamycin) were reported to function as covalent molecular glue degraders that targeted Cys374 of the putative E3 ligase UBR7 and promoted interactions with the neosubstrate tumor-suppressor TP53.[20]

Synthetic molecular glue degraders

Molecular glue degraders for $CRL4^{CRBN}$. The pivotal study of Ito *et al.* in 2010 described the first identification of a synthetic molecular glue degrader's mechanism of action. Using affinity purification of HeLa cell extracts with thalidomide-coated beads, followed by experiments in zebrafish and chicken models, they identified cereblon (CRBN), the substrate receptor of the CUL4-RBX1-DDB1-CRBN ($CRL4^{CRBN}$) E3 ubiquitin ligase as the molecular target of the drug thalidomide.[21] Thalidomide was prescribed in West Germany in 1957 as an anti-emetic and sedative to pregnant women but was withdrawn from the market in 1962 due to its teratogenic side-effects.[22] Currently, thalidomide and its analogs (pomalidomide, lenalidomide, also known as immunomodulatory drugs, IMiDs, or CRBN E3 ligase modulatory drugs, CELMoDs) are used in multiple myeloma and other hematologic malignancies. In 2014, key structural studies by Chamberlain *et al.*[23] and Fischer *et al.*[24] elucidated the architecture of the ternary complexes of lenalidomide, thalidomide and pomalidomide with CRBN-DDB1 (DNA damage binding protein-1, an adaptor protein component of the DDB1–CUL4–Rbx1 ubiquitin ligase (CRL4)) (Fig 1A). Crystallographic data showed that IMiDs bound on the surface of CRBN in a shallow, hydrophobic pocket, comprising three tryptophan residues (Trp380, Trp386, Trp400). This shallow pocket accommodated the glutarimide ring, which formed hydrogen bonds with His378 and Trp380 (CRBN). The isoindolinone ring was exposed on the surface of the CRBN–lenalidomide complex, implicating this moiety in the formation of a neomorphic interface for substrate recruitment. Upon binding to CRBN, IMiDs inhibited the ubiquitination of the endogenous $CRL4^{CRBN}$ substrates and at the same time reprogramed the ligase to target new proteins for degradation. IMiDs promoted neomorphic interactions with the C_2H_2-type zing-finger transcription factors Ikaros (IKZF1) and Aiolos (IKZF3) leading to their ubiquitination by the E3 ligase $CRL4^{CRBN}$ and subsequent proteasomal degradation.[25–27]

Follow-up studies showed that IMiDs had distinct degradation profiles[28] and could recruit different neosubstrates, including casein kinase 1A1 (CK1α) and the translation termination factor GSPT1. Crystallographic studies supported the hypothesis that the specificity in the formation of neomorphic interactions was indeed dictated by the solvent-exposed area of the compound in the IMiD/CRBN-binary structure. The crystal structure of lenalidomide/DDB1-CRBN/CK1α showed that the binding was cooperative, since CK1α binding to CRBN was strictly dependent on the presence of lenalidomide.[29] CRBN and lenalidomide provided the binding interface for a CK1α β-hairpin-loop located in the kinase N-lobe. In addition to the previously described interactions with CRBN, CK1α interacted with the solvent exposed part of the compound via residues Ile37, Thr38 and Gly40 (Fig 1A). In the case of CC-885, a novel CRBN modulator with improved anti-tumor activity[30] GSPT1 was recruited to $CRL4^{CRBN}$ and degraded. Crystallography showed that CC-885 maintained the key interactions with CRBN and additional

interactions were formed with Glu377 (CRBN), Val570 and Gly575 (GSPT1), as well as direct interactions between CRBN and GSPT1, allowing the identification of the residues involved in the recruitment of GSPT1 (Fig 1A). The crucial feature that mediated the GSPT1 binding to CRBN was a surface turn containing the key glycine residue (Gly575). A CRBN modulator with improved degradation of Ikaros and Aiolos, CC-220 was also reported.[31] A similar binding mode to CRBN was observed from the glutarimide ring (Fig 1A), whereas the additional rings, in the solvent exposed area, formed more interactions with CRBN (Glu377, Pro352, Phe102, Phe150) and these additional interactions correlated with the observed increased affinity to CRBN.

Collectively, the observations for the recruitment of seemingly diverse neosubstrates by the IMiDs led to the degron hypothesis.[28–30] Despite the fact that Ikaros, Aiolos, CK1α and GSPT1 were structurally and functionally unrelated and lacked an obvious sequence homology, the presence of a homologous interacting structural feature (degron), defined by a specific loop containing a glycine residue at a key position, was sufficient for their recruitment. Mutation of the key glycine to alanine resulted in loss of function. Further studies revealed that the IMiDs disrupted a broad transcriptional network by degrading several C_2H_2 zinc finger transcription factors[32] and the human C_2H_2 zinc finger degrome was defined.[33] The teratogenic effects of thalidomide and its metabolite, 5-hydroxythalidomide, were associated with its induced degradation of the embryonic transcription factor SALL4.[34] The crystal structure of SALL4-pomalidomide-CRBN-DDB1 was solved shortly thereafter and provided the rational basis for designing IMiDs with reduced teratogenic risk.[35]

Rational optimization of novel CRBN modulators has led to a new generation of IMiDs/CELMoDs. Two CELMoDs (CC-3060 and CC-647) targeting the transcription factor ZBTB16 were reported in 2020.[36] Interestingly, the two compounds recognized distinct structural degrons within different zinc finger domains (1 and 3) of ZBTB16. The discovery of CC-92480 followed.[37] CC-92480 is a CELMoD specifically designed for efficient and rapid degradation kinetics, and is currently in clinical trials for multiple myeloma. Improved GSPT1 degraders with increased potency and selectivity, such as ZXH-1-161[38] and CC-90009[39] were also reported. CC-90009 was the first clinical candidate to selectivity target GSPT1. Structurally, CC-90009 showed similarities with the binding mode of CC-220, including interactions with both with CRBN and GSPT1. A notable structural difference was the lack of interaction with Glu377 (CRBN) and instead a new bond was formed with His353 (Fig 1A). Together, these crystallographic studies were fundamental for defining the binding mode of IMiDs to CRBN and its neosubstrates and for establishing rational drug development based on the degron hypothesis.

In 2022, a groundbreaking study by Watson *et al.*[40] showed that IMiD/ CELMoD compounds regulated the conformation of cereblon. Cryo-electron microscopy (cryo-EM) was used to compare the apo complex of DDB1-CRBN to the structure of CELMoD-DDB1-CRBN with or without neosubstrates. Binding of CELMoDs to CRBN's thalidomide-binding domain (TBD) was sufficient to induce an allosteric rearrangement of CRBN from an open conformation to the closed conformation seen in the crystal structures. The closed conformation observed in the crystal structures with CELMoD enabled the structure-guided optimization of CELMoDs towards more potent and more-neosubstrate specific compounds. Remarkably, in the cryo-

EM studies, Ikaros associated only with the closed CRBN conformation. Three compounds [pomalidomide, iberdomide (CC-220), and mezigdomide (CC-92480)] had distinct effects on the observed conformations of CRBN, which correlated with the compounds' potency. Pomalidomide was sufficient to induce the closed conformation of CRBN for only ~20% of the particles. Iberdomide, which has ~20-fold improved affinity and ~24-fold enhanced Ikaros degradation, shifted nearly 50% of the particles to the $CRBN^{closed}$ conformer. For mezigdomide, which induced rapid neosubstrate degradation and was efficacious in relapse or refractory patients who no longer responded to primary treatment with lenalidomide and/or pomalidomide, 100% of the particles were in the closed conformation (Fig 1A). The study thus elucidated the cryptic role of allostery and the significance of conformational control for CRBN molecular glue degraders, allowing further rational designs of MGDs with improved neosubstrate selectivity and efficacy.

Molecular glue degraders of RBM39 (recruiting $CRL4^{DCAF15}$). After the IMiDs/ CELMoDs, the second type of molecular glues discovered to recruit neosubstrates to an E3 ligase were the splicing inhibitor sulfonamides [SPLAMS: indisulam, tasisulam, E7820 (NSC 719239) and chloroquinoxaline sulfonamide (CQS or NSC 339004)] (Fig 1B). In 2017, two groups reported that SPLAMS promoted the recruitment of RBM39 (RNA binding motif protein 39, also known as CAPERα) to the E3 ubiquitin ligase CUL4–RBX1–DDB1–DCAF15 ($CRL4^{DCAF15}$), leading to RBM39 polyubiquitination and proteasomal degradation[41,42].

Extensive biochemical and structural studies, including ternary complexes solved by crystallography and two cryo-EM structures, were reported in 2019[43,44] and 2020[45] and elucidated the molecular-glue mechanism of action. These studies showed that the sulfonamides had low binding affinity for the individual proteins and emphasized the structural complementarity of the sulfonamides with the ternary complexes. For example, indisulam's K_i was > 50 μM for the DCAF15–DDB1–DDA1 complex, whereas its binding affinity in the presence of RBM39 decreased to 187 nM, a >100-fold enhancement (determined by ITC). In all three structural studies, the aryl sulfonamides bound synergistically, promoting the binding of DCAF15 to the RNA-recognition motif (RRM) of RBM39 ($RBM39_{RRM2}$) and forming a stable ternary complex by functionalizing a shallow, non-conserved cavity on the surface of DCAF15 (Fig 1B). The binding and recruitment of RBM39 to the DCAF15-sulfonamide interface was mediated through a single α helix of RBM39, which interacted with DCAF15-sulfonamide through both main-chain carbonyl oxygens and side chains. The large total buried surface area of the $RBM39_{RRM2}$–DCAF15 PPI (1,150 $Å^2$) was able to compensate for the weak binding affinity of the compounds to DCAF15 alone. The aryl sulfonamide moiety, common to all reported RBM39 degraders, formed hydrogen bonds with the main chains of Ala234 and Phe235 of DCAF15 via the oxygen atoms. Water-mediated hydrogen bonds were formed with Thr262 and Asp264 of RBM39 via the nitrogen atom of the sulfonamides. Additionally, an extensive non-polar, hydrophobic network between DCAF15-RBM39 sidechains led to the high-affinity ternary complex. Notably, in cryo-EM structures, DCAF15 engaged the second RRM domain of RBM39 with an extended, non-conserved surface area not commonly observed in CRL (Cullin-Ring E3 ligases) substrate receptors. The selectivity implied by the positioning of DCAF15 and the binding mode in the ternary complexes was further validated with mass spectrometry (MS)-based proteomic experiments for E7820 to determine its

degrome. Other than RBM39, only RBM23 with 100% sequence identity across all interacting residues was degraded out of the ~11,000 proteins detected.

In 2020, Mayor-Ruiz *et al*, reported a scalable chemical profiling approach as a rational strategy for the discovery of molecular glue degraders using an E3-ligase agnostic approach.[46] The strategy took advantage of the requirement for neddylation of CRLs to become activated, by comparing the sensitivity of hyponeddylated (UBE2M^{mut} KBM7) vs neddylation-proficient (KBM7) cells to compound-mediated cell death. Screening ~2,000 cytostatic/cytotoxic small molecules both in wildtype and UBE2M^{mut} KBM7 cells, led to the identification of chemical scaffolds that appeared to be functionally dependent on uninterrupted neddylation levels. Among them a novel sulfonamide, dCeMM1 was identified to reprogram the CRL4^{DCAF15} ligase and selectively degrade RBM39, sparing RBM23.

Excitingly, the MGDs targeting CRL4^{DCAF15} differed from the IMiDs in chemical structure, E3 ligase target, neosubstrate structure, and size of the PPI interface. The existence of two entirely distinct classes of MGDs suggested that molecular glues could be everywhere if one knew how to look for them.

Molecular glue degraders for cyclin K. Another successful approach to discover new MGDs focused on known inhibitors to identify a suspected missing degradation component. In 2020, three independent and nearly simultaneous studies reported structurally diverse small molecules that induced the degradation of cyclin K. Słabicki *et al*.[47] hypothesized that a cytotoxic compound could demonstrate cell-line selectivity based on the expression a required-but-unidentified ubiquitin-ligase component. They performed systematic database mining to correlate the cell-line sensitivity of 4,518 clinical and preclinical small molecules with the respective mRNA levels of E3 ligase components across 578 human cancer cell lines. They observed a correlation between the cytotoxicity of a cyclin-dependent kinase (CDK) inhibitor, CR8, and the mRNA levels of the CUL4 adaptor protein DDB1. Further mechanistic studies proved that CR8 acted as a molecular glue degrader by inducing the formation of a complex between CDK12/cyclin K and DDB1. It is noteworthy that DDB1+CDK12 formed a weak protein complex with a large, structurally complementary interface (2,100 Å^2) with a basal affinity of ~50 µM in ITC experiments. CR8 enhanced the interaction by 500-1000-fold (K_d = 100-500 nM). Structurally, CR8 occupied the ATP binding site of CDK12, bridging the CDK12-DDB1 interface and forming discrete contacts with one of the beta propeller domains of DDB1 (Fig 2A). The key structural feature on CR8 was the hydrophobic phenylpyridine ring system, which was solvent exposed on the kinase surface and induced the complex formation with the ligase adaptor DDB1 by interacting with Arg928 (DDB1). Cyclin K bound on the opposite face of CDK12 and did not interact directly with DDB1. Notably, CDK12 is not a constitutive E3 ligase component. Structure-guided mutational analyses and TR-FRET assays showed that in the presence of CR8, CDK12 assumed the role of a glue-induced substrate receptor and placed cyclin K in a position typically occupied by CRL4 substrates; thus, binding was mutually exclusive with a canonical DCAF substrate receptor. The authors rigorously proved that CR8, a promiscuous kinase inhibitor, was a selective cyclin K degrader.

Using a different approach, Mayor-Ruiz *et al*.[46] established a comparative chemical screening assay in hyponeddylated cellular models with broadly abrogated ligase activity. As described above, the strategy

was validated by the identification of the sulfonamide dCeMM1 that degraded RBM39. Additionally, three small molecules (dCeMM2/3/4) were identified as dependent on functional CRLs to exert their toxicity. Cellular treatment and quantitative expression proteomics showed that dCeMM2/3/4 profoundly destabilized cyclin K and more mildly destabilized the associated kinases CDK12 and CDK13. Further validation with orthogonal assays, including quantitative proteomics, functional genomics, drug-affinity chromatography, and cellular proximity assays, revealed the compound-induced association of CDK12-cyclin K and DDB1-CUL4B.

At the same time, Lv *et al.*[48] reported a high-throughput phenotypic screening approach for NRF2 inhibitors that surprisingly led to the identification of HQ461, a molecular glue degrader of the same CDK12/cyclin K/DDB1 complex. Gain-of-function screening based on hypermutation, CRISPR-cas9 screening, biochemical assays, and cross-linking confirmed the glue-type mechanism of action.

In 2021, Dieter *et al*.[49] reported a high-throughput screen of a library consisting of 80,000 small molecules without known activity against a heterogeneous collection of patient-derived metastatic colorectal cancer (CRC) spheroids. Follow-up transcriptomics and chemical proteomics validated compound NCT02 as a molecular glue that induced the ubiquitination of cyclin K and the proteasomal degradation of its partner, CDK12. A notable difference from CR8 was the lack of detectable CDK12 kinase inhibitory activity for NCT02.

In 2022, Jorda *et al.*[50] reported a series of 3,5,7-substituted pyrazole[4,3-*d*]pyrimidine based inhibitors of CDKs. Among them, compound 24 induced the degradation of cyclin K. Molecular docking studies suggested a similar binding mode to CR8. It must be noted that with the exception of the crystal structure of CR8, no crystal structures for the other cyclin K degraders were reported in the original studies.

A remarkable observation from these studies was the structural diversity of the compounds that degraded cyclin K with the same molecular-glue mechanism of action. In 2023, Kozicka *et al.*[51] thoroughly investigated the structure-activity relationships (SAR) of cyclin K degraders. Over 90 structurally diverse compounds were evaluated; first in vitro using a TR-FRET assay that measured complex formation between CDK12–cyclin K and DDB1 in the presence of small molecules, and then in cellular assays. 40 of these compounds showed low nanomolar affinity (<100 nM in vitro) for the CDK12-DDB1 complex and the structures of 28 ternary complexes were solved by crystallography (Fig 2A). The role of Arg928 in DDB1 as a hotspot residue for gluing moieties was confirmed. The glues targeted Arg928 preferentially with π-cation interactions, and in some cases via hydrogen bonds and hydrophobic interactions. Overall, arenes and heteroarenes with varying sizes, and even weaker aliphatic groups were able to engage with Arg928 and enabled CDK12/DDB1 interactions. Appropriate electronic and steric effects for π-cation interactions with DDB1 were crucial for forming a high-affinity complex. Notably, the purine moiety interacting with the hinge kinase residues (Met816, Glu814, Tyr815 in CDK12) was unable to enhance gluing activities independently, but only synergistically in cases that the Arg928 (in DDB1) was appropriately targeted. Even smaller analogs – as exemplified in compound 919278 – that lacked the typical purine-based kinase inhibitor moiety were able to form sufficient interactions with the kinase hinge residues and Arg928, thus

acting as molecular glue degraders. These observations demonstrated that a minimal pharmacophore fingerprint for cyclin K degraders was the hinge-interacting acceptor–donor motif, which is common for kinase inhibitors, and an additional gluing moiety including an aromatic system extending from the hydrogen bond donor.

Thorough cellular validation and characterization of the compounds followed and included reporter assays, viability assays, kinase inhibitory profiling, proteomics, and RNA-seq. An important observation was that the inhibiting versus degrading functions were directly tunable and could largely be decoupled, especially when small compounds with no inhibitory activity were used as starting points for the development of degraders. The ubiquitination and subsequent degradation of cyclin K further required additional compound-mediated interactions. The authors also noted that the biochemical ternary affinity was predictive of degradation in cellular systems.

The structural diversity of cyclin K degraders and tolerant SAR were linked to the large, complementary PPI interface in this case, where the degraders contributed to ~20% of the binding surface. The identified glues showed specificity for CDK12 and CDK13, whereas other kinases were not targeted. The specificity for the CDK12/cyclin K complex or the structurally similar CDK13/cyclin K could be explained by the unique CDK12/13 C-terminal tail that contributed to the neomorphic PPI interface. As a more general conclusion, the authors proposed that structure-activity relationships and substrate specificity correlated with the absolute size of the PPI interface, as well as the relative contribution of the compound to the interface. From a discovery perspective, the diverse screening approaches that uncovered the same CDK12/DDB1 complex encourages future innovation.

Degraders of β-catenin. In 2019, Simonetta *et al.* described the identification and rational design of molecular glues that restored the native PPI between the oncogenic transcription factor β-catenin and its cognate E3 ligase, $SCF^{\beta\text{-}TrCP}$.[52] The WNT pathway is often dysregulated in cancer, with diverse mechanisms leading to reduction in β-catenin phosphorylation at the phosphodegron residues Ser33 and Ser37. Loss of phosphorylation impairs its ability to effectively bind to $SCF^{\beta\text{-}TrCP}$ and prevents its degradation. A fluorescence polarization (FP) binding assay was developed utilizing β-catenin phosphodegron residues and recombinant β-TrCP/Skp1 complex (referred as β-TrCP subsequently). The binding affinity of singly phosphorylated peptide (phospho-Ser33/Ser37) was more suitable for the development of an HTS assay than unphosphorylated or phospho-Ser37 peptides. Screening a 350,000-compound library led to the identification of four structurally similar compounds, including NRX-1532. The compound was further validated with TR-FRET and SPR assays. The crystal structure of the ternary complex of β-catenin/β-TrCP/NRX-1933, a structurally similar but more soluble tetrazole analog, was solved (Fig 2B). The compound bound in the PPI interface and formed interactions with both partners. The trifluoromethylpyridone group filled an additional small hydrophobic pocket that was revealed due to the absence of Ser37 phosphorylation and acted as a phosphate mimic. The TR-FRET assay further supported the cooperative binding mode.

The crystal structure b-factors suggested that the N-terminus of the β-catenin peptide was not tightly bound and could potentially reveal a larger and more druggable binding pocket. This hypothesis was tested with compounds such as NRX-2633 that included a phenoxy substituent and were able to induce the rearrangement of Leu31, thus creating a larger pocket. NRX-2633 showed improved potency in the binding assay and enhanced cooperativity (13-fold). Structure-guided optimization of the phenoxy substituent to diarylthioethers led to analogs NRX-252114 and NRX-252262 with significant improvements in both potency (EC_{50} values of 6.5 nM for NRX-252114 and 3.8 nM for NRX-252262; an improvement of >10,000-fold) and cooperativity (>1500-fold), compared to the screening hit. The two compounds were further evaluated in cell assays and were able to potentiate the binding of S37A mutant β-catenin to β-TrCP, increase K48-linked ubiquitination of mutant β-catenin and restore its proteasomal degradation.

The study highlights the importance of cooperativity since the molecular glues bind to the ternary complex but not to β-TrCP alone. An important advantage of restoring a native PPI with molecular glues, as showcased here, is that there is a naturally occurring interface and accessible lysine residues on the substrate for ubiquitination and degradation. Additionally, the molecular glues were selective for the mutant form of β-catenin; thus, the wild-type function in normal tissues should not have been affected by this strategy. This work represents the first rational example of molecular glues targeting native substrate–E3 ligase interactions. The strategy could be applied to other native PPIs weakened by mutations at the PPI interface. The β-catenin example also highlights a potential pitfall for biochemical screening for weak PPIs; namely, if binding is too weak to detect, it can be difficult to develop the assay and biological relevance could be compromised.

Non-degradative molecular glues / PPI stabilizers

Natural products

Several classes of natural products stabilize PPIs without leading to the degradation of either protein. Among these are the well-studied examples of rapamycin and microbial macrolides, such as FK506 and cyclosporin A. In all three cases, the MG mechanism of action was discovered retrospectively. Cyclosporin, an immunosuppressive agent, binds to cyclophilin and calcineurin, a Ca^{2+}/calmodulin-dependent protein phosphatase.[53] Upon formation of the ternary complex, the phosphatase activity of calcineurin is inhibited, leading to activation of interleukin-2. Calcineurin is also the target of microbial macrolides, like FK506 (also known as tacrolimus), which simultaneously binds to FK506-binding protein 12 (FKBP12) and calcineurin. The formed ternary complex reduces the activity of the peptidyl-prolyl cis-trans isomerase of FKBP12 and the phosphatase activity of calcineurin. Rapamycin, a potent immunosuppressive agent, binds simultaneously to two proteins: the FK506-binding protein (FKBP12) and the FKBP-rapamycin-associated protein (FRAP), also known as the mechanistic target of rapamycin (mTOR). The crystal structures of FK506/FKBP12/calcineurin in 1995[54] and rapamycin/FKBP12/FRAP in 1996[55] are the first examples of ternary complexes of molecular glues. In both cases, the natural products form extensive ligand-protein interactions with both protein partners and contribute to 25-50% of the total buried surface area.

14-3-3 PPI stabilizers. Another important class of non-degradative natural product MGs are the fusicoccanes. Fusicoccin-A (FC-A) and cotylenin-A stabilize native PPIs between the scaffolding, adaptor protein 14-3-3 and its clients.[56–59] 14-3-3 proteins have a very extensive interactome that includes tumor

promoters, tumor suppressors and transcription factors. 14-3-3 exerts its functions by recognizing and binding to short phospho-serine/threonine (pS/pT) motifs on intrinsically disordered domains/regions of the client protein.[60,61] Binding of 14-3-3 to its clients leads to diverse biological effects depending on the localization, function, and role of the client. For transcription factors, such as ChREBP[62] and estrogen receptor alpha (ERα)[56], binding to 14-3-3 has an inhibiting effect, controlling their shuttling between the nucleus and the cytoplasm. Modulating the native interaction between 14-3-3 and ERα by FC-A inhibited ERα binding to DNA and reduced cell growth in ERα-dependent cell lines. Thus, 14-3-3/ERα stabilization may be an alternative therapeutic strategy for breast cancer treatment, where mutations often occur in the ligand-binding domain of ERα. 14-3-3 is also a central regulator of the MAP kinase signaling pathway, where it has a dual role.[63–67] As a dimeric protein, 14-3-3 maintains RAF kinases in an inhibited state by interacting with two RAF phosphorylation sites (pS259 and pS621 on C-RAF). Upon pathway activation, interaction with RAS and dephosphorylation of the inhibiting pS259 site, conformational changes occur that allow the dimerization of two RAF's kinase domains bound to one 14-3-3 dimer. The active RAF homo- or heterodimers promote MAP kinase signaling. Thus, the stabilization of the 14-3-3/RAF inhibitory complex offers an alternative approach to modulate the MAPK pathway, often dysregulated in cancers and in certain developmental disorders, instead of direct RAF inhibition.

Although the underlying biology of 14-3-3 is well understood for several targets, and the potential advantages of a therapeutic intervention are enticing, the complex nature of the natural product stabilizers makes them unsuitable for further clinical advancement. Nevertheless, fusicoccanes were significant in proving the ligandability of the site. Diverse approaches have since been disclosed for the identification of client-specific 14-3-3 stabilizers, including virtual screens,[68] high throughput screens,[69,70] and fragment-based approaches.[71–75] In each case, the screens utilized a phosphopeptide derived from the client protein, since the disordered domains of client proteins are often difficult to isolate recombinantly. Here, we describe a few representative examples in more detail (Fig 3A). Although the 14-3-3 stabilizers are not as preclinically advanced as some of the MGs described above, the focus of these studies has been to develop a systematic discovery-and-optimization framework for molecular glues; this rational, structure-guided approach may expose underlying principles for MG discovery more broadly.

A targeted virtual screening approach was used to identify stabilizers of the 14-3-3/ChREBP complex. ChREBP (carbohydrate-response element-binding protein) is a glucose-responsive transcription factor that plays an important role in the pathogenesis of glucolipotoxicity.[62,68] 14-3-3 binding to ChREBP results in its cytoplasmic retention and suppresses its transcriptional activity. Stabilization of this interaction could therefore be therapeutically useful for type 2 diabetes. ChREPB is one of the few phosphorylation-independent 14-3-3 binding proteins and binds to 14-3-3 in a unique α-helical conformation.[76] The pS/pT site in the composite PPI interface can accommodate a free sulfate, phosphate, or adenosine monophosphate (AMP). The screening of phosphonate analogs, which typically inhibit the 14-3-3/ChREPB PPI, resulted in the identification of one PPI stabilizer, which was rationally optimized further. The optimized compound 3 stabilized the 14-3-3/ChREBP complex by 14-fold in fluorescence anisotropy titrations. The ternary crystal structure showed that this phosphonate MG bound cooperatively in the phospho-accepting 14-3-3 pocket and formed multiple interactions both with 14-3-3β and the ChREBP

peptide (Fig 3A). Polar interactions were formed with 14-3-3β (Lys51, Arg58, Arg129, Tyr130) and ChREBP (Arg128). Hydrophobic interactions were also observed between the phenyl ring of compound 3, 14-3-3 (Leu218, Ile219, Leu174, Leu222) and ChREBP (Ile120). The phosphonate group of compound 3 formed polar interactions with Arg128 (ChREBP), which further interacted with Glu182 (14-3-3), thus locking the conformation of this ChREBP residue. Further optimization of the stabilizers allowed their evaluation in a cellular setting, where they showed retention of ChREBP in the cytoplasm and repression of ChREBP transcriptional activity.[77]

Fragment-based screens utilizing different technologies have been particularly robust for discovering 14-3-3/client stabilizers. Fragments, due to their small size, provide useful starting points for targeting the complex protein surfaces typical of PPI interfaces[78]. The peptide-binding groove on 14-3-3 is largely conserved but the sequence and conformation of the client phosphopeptide varies dramatically from client-to-client. Thus, the shape and amino-acid composition at the FC-A binding site in the formed 14-3-3/client complexes are highly divergent, allowing the selective targeting of 14-3-3/client PPIs. Furthermore, different residues on 14-3-3 can be targeted as 'anchor' binding elements. For instance, imine-based tethering approaches have been reported for the 14-3-3/p65[73] and the 14-3-3/PIN1 complexes.[79] Aldehyde-containing fragments that bound to the conserved Lys122 of 14-3-3 in the middle of the binding groove, showed weak stabilization of the 14-3-3/p65 complex by adopting a conformation that facilitated interactions with the p65 peptide. In a similar manner, optimized aldehyde-containing compounds, such as compound 23, stabilized the 14-3-3/PIN1 complex via specific pi-pi interactions with the tryptophan of the PIN1 peptide (+1 position of the phospho-site) (Fig 3A).

The ease of crystallization of 14-3-3/phosphopeptide complexes has facilitated structure-guided fragment-linking approaches. A crystallographic screen identified amidine fragments that bound via an anchoring ionic bond to Glu14 of 14-3-3 at the rim of the interface.[71] The fragments stabilized either the 14-3-3/TAZ or 14-3-3/p53 complexes with distinct binding modes in each case. A second fragment, targeting an engineered cysteine at Asn42Cys mutation on 14-3-3 was identified using intact mass spectrometry (disulfide tethering)[72]. The disulfide tethering technology relies on the formation of reversible disulfide bonds between the fragment and native or engineered cysteines.[80] A tethering screen of 1600 disulfide fragments identified compounds that bound preferentially in the presence of the ERα-derived phosphopeptide.[72] Co-crystallization demonstrated a favorable positioning of this tethered fragment next to the previously identified amidines, enabling a fragment-linking approach for the development of non-covalent 14-3-3/ERα stabilizers.[81] The optimized compound 24 stabilized the 14-3-3γ/ERα complex by 25-fold in fluorescence anisotropy (FA) titrations. The binding mode and the interacting amino acid residues at the interface are shown in figure 3A.

Disulfide tethering screens were also targeted to a cysteine residue on a phosphopeptide client (ERRγ[75]) and to the native Cys38 found in 14-3-3σ at the periphery of the binding groove.[74] In the latter case, comparative disulfide tethering screens with 14-3-3-binding phosphopeptides with diverse shapes and binding modes (ERα, C-RAF, FOXO1, USP8, SOS1) identified both non-selective and client-selective disulfide stabilizers. The binding mode of a C-RAF selective fragment (fragment 7) is shown in figure 3A. It

is noteworthy that the diversity of the 14-3-3/client interfaces led to a diversity of hits, suitable for further structure-guided optimization.

A non-selective fragment (fragment 1) was found to stabilize both the 14-3-3σ/ERα and 14-3-3σ/CRAF complexes, with a stronger preference for C-RAF. Fragment 1 was used as a starting point for the development of irreversible, covalent stabilizers of the 14-3-3σ/ERα complex via structure-guided optimization.[82] Although the binding mode of the fragment was similar in both cases, the two client phosphopeptides were vastly different. ERα bound to 14-3-3 via Val595 at the C-terminus of ERα, whereas C-RAF bound with an internal sequence centered on phospho-Ser259. Chemical modifications of the fragment included the replacement of the disulfide tether with irreversible electrophiles, modifications in close proximity to the 14-3-3/ERα interface, aiming for specific interactions with both, and conformational locking of the warhead at the rim of the interface with spiro-cycles. The overall optimization tuned the selectivity towards ERα, and a minimal effect was observed for C-RAF due to steric hindrance. Compound 181 showed strongly enhanced potency and cooperativity in biophysical assays, similar to the FC-A natural product ($app K_d$ for the 14-3-3/ERα peptide complex was 18 nM, a 116-fold stabilization at 100 μM compound). In the crystal structure, 181 bound covalently to Cys38 (14-3-3) and formed water-mediated hydrogen bonds with Arg41 (14-3-3) and Asp215 (14-3-3) at the rim of the interface (Fig 3A). At the protein/peptide interface, the *p*-chloro-aniline moiety formed a halogen with Lys122 (14-3-3). A water network was formed between the oxygen of the tetrahydropyran, the terminal carboxy group of ERα and the NH group of the aniline. Hydrophobic interactions were observed between the methyl group and the shallow, hydrophobic pocket formed by 14-3-3 residues (Leu218, Ile219, Leu222). The presence of the spiro-cycle locked the overall conformation of the complex, resulting in high shape complementarity in the binding pocket and significantly improved cooperativity over more flexible analogs. In cell-based ERα luciferase reporter assays, compound 181 reduced ERα transcriptional activity more effectively compared to the natural product and blocked breast cancer cell proliferation. In western blots, compound 181 increased phosphorylation levels of the ERα Thr594, indicating that it enhanced binding of 14-3-3 to its ERα phospho-site, thereby protecting it from phosphatases.[77]

These 14-3-3/client stabilizers demonstrate that the rational identification of molecular glues for diverse, native PPIs can be achieved via different screening approaches. These approaches are likely applicable to other targets beyond 14-3-3, and bear resemblance to the β-catenin example described above. Despite the common binding site on the 14-3-3/client binding grove, selective molecular glues can be developed by targeting the +1 peptide residue adjacent to the phospho-site of the client, which is significant for molecular recognition, and at the same time aiming at the chemically unique composite binding pocket formed by a given 14-3-3/client PPI interface. The 14-3-3/client MGs, as exemplified in the crystal structures of the ternary complexes, form interactions with both partners. Additionally, they show low or no intrinsic affinity to the individual binding partners and act cooperatively via enhancing the existing affinity of the native PPIs. Covalently bound 14-3-3 MGs also bear resemblance to the cereblon-binding IMiDs. In both cases, the binding to the 'hub' protein is consistent, and diversification of the client-binding side of the compound provides specificity. Full-length structures of cereblon, however, demonstrate large

conformational changes that also drive ternary complex formation; it remains to be seen whether full-length ternary complex structures for 14-3-3/client/MGs also show long-range interactions.

Using 14-3-3/client complexes as examples, de Vink *et al.* have described a cooperativity model[57] to quantify the efficacy of PPI stabilizers in terms of the cooperativity factor (α) between the stabilizer and the binding partners, as well as the intrinsic affinity of the stabilizer towards one of the apo-proteins (K_D^{II}) (Fig 3B). The cooperativity framework relies on fluorescence polarization measurements (2D-FP protein titrations) and a semi-numerical thermodynamic model based on the sequential binding of protein (R) or phosphopeptide partner (P) and stabilizer (S). The binding partner binds to the target protein with K_D^{I}. In the presence of stabilizer, the enhanced affinity becomes K_D^{I}/α. When the partner is already bound to the target protein the K_D^{II} in the presence of stabilizer is enhanced to K_D^{II}/α. The model allows the development of structure-activity relationships, and the efficacy of the stabilizers is attributed to either changes in cooperativity or intrinsic affinity.

Trametinib: a stabilizer of the MEK/KSR PPI. An unexpected molecular-glue type interaction for a native PPI was reported for the MEK inhibitor trametinib. In 2020 Khan *et al.* solved crystal structures of MEK bound to the pseudokinase KSR (kinase suppressor of RAS) in the presence of MEK inhibitors[83] (Fig 3C). Among them, the FDA-approved drug trametinib directly engaged KSR at the MEK interface, in a molecular glue type ternary complex. Trametinib, as an ATP-noncompetitive kinase inhibitor, occupied the typical MEK inhibitor allosteric site adjacent to ATP, but its 3-substituted phenyl acetamide group also extended into a sub-pocket that reached the KSR interaction interface. This phenyl acetamide was unique to trametinib compared to other clinical MEK inhibitors. The moiety occupied a pocket formed at the MEK-KSR interface and formed contacts with both proteins. Trametinib also disrupted the RAF-MEK complex due to a putative steric clash between the phenyl acetamide and the pre-helix αG loop in BRAF. The structural information was then used to design a compound imaginatively called trametiglue, to test whether adaptive resistance to MEK inhibitors could be overcome by alterations at the interfaces of KSR-MEK and RAF-MEK. Trametiglue had a sulfamide group instead of the acetamide group of trametinib and this allowed the formation of two additional hydrogen bonds at the interface of KSR-MEK. Co-immunoprecipitation assays showed that trametiglue, but not trametinib, markedly enhanced capture of BRAF, suggesting a favorable binding of BRAF to MEK. This strategy could be further applied to the rational design of MEK inhibitors by targeting the interfacial binding regions of regulatory complexes in the MAPK pathway with MG-type molecules.

LSN3160440: a stabilizer of GLP-1R/GLP-1 PPI. In 2020 Bueno *et al*. reported the discovery of LSN3160440, a molecular glue that stabilized an active-state conformation of a G-protein coupled receptor (GPCR) by binding cooperatively both to the receptor (GLP-1R) and to an orthosteric ligand [GLP-1-(9-36)].[84] GLP-1-(9-36), a metabolite of the native ligand GLP-1(7-36), although functionally inactive, retains weak affinity to GLP-1R. A 220,000-compound library was screened using GLP-1R expressing HEK293 cells in the presence of GLP-1-(9-36) at EC_{20} (20% maximum effective concentration) to identify allosteric modulators. Multiple cycles of SAR optimization of the hits led to compound LSN3160440, which enhanced both the potency and relative efficacy of GLP-1-(9-36). The complex of GLP-1R bound to LSN3160440 with full-

length GLP-1, heterotrimeric G_s, and the camelid antibody Nb35 was determined using cryo-EM (Fig 3D). LSN3160440 bound to the extracellular side of GLP-1R in a pocket formed at the interface of transmembrane helices TM1 and TM2. Ligand-receptor and ligand-peptide interactions were also formed at the TM1-TM2 interface. Thus, LSN3160440 bound to GLP-1R and GLP-1 simultaneously, stabilizing a new interface and potentiating the intrinsic activity of GLP-1(9-36) to fully activate the receptor. LSN3160440 represents the first example of a PPI stabilizer affecting cell surface signaling.

Molecular glues inducing self-association

In contrast to native PPI stabilizers, there are numerous examples of compounds that induce self-association, including homo- or heterodimerization, oligomerization or polymerization of the target protein. In most of the cases, the molecular glue-type self-association mechanism of action was discovered retrospectively. One striking contrast is the biophysically based, prospective discovery of Tafamidis[85], which stabilizes the tetramer of transthyretin, inhibiting its dissociation and aggregation. Tafamidis is used to treat patients with transthyretin familial amyloid polyneuropathy (TTR-FAP), a rare autosomal dominant neurodegenerative disorder. In the 2000's, the Kelly lab determined that the rate-limiting step in transthyretin amyloid formation was the dissociation of the tetramer to monomers; by kinetically stabilizing the tetramer with a small molecule 'chaperone,' they were able to slow dissociation and inhibit amyloid formation. The discovery of Tafamidis represented a rational, structure-based drug design effort that led to a first-in-class therapeutic agent, and furthermore paved the way for discovering new oligomer-stabilizing molecular glues.

BCL6 degraders. Development of BCL6 (B-cell lymphoma 6 protein) inhibitors is one of the most-well known recent examples of compounds leading to high-order polymerization. These compounds could also be classified as MGDs, but the feature of high-order polymerization makes them in a way distinct from the MGDs described earlier. The transcription factor BCL6 is involved in lymphoid malignancies and non-Hodgkin lymphomas, including diffuse large B cell lymphoma (DLBCL). BCL6, as a transcriptional repressor, binds specific DNA sequences via zinc fingers (ZF) and recruits transcriptional co-repressor complexes via its BTV/POZ domain. The BTB domain, a protein interaction motif at the N-terminus, forms an intertwined head-to-tail homodimer and can adopt various oligomeric states. In 2017, Kerres *et al.* showed that the BTB domain of BCL6 was highly druggable and performed structure-based drug design to identify inhibitors.[86] A high-throughput screen by fluorescence polarization (FP) was performed with a library of 1,700,000 compounds monitoring the interaction of a co-repressor peptide with the BTB domain of BCL6. The hits were further validated with surface plasmon resonance (SPR), crystallography, and a biochemical ULight co-repressor peptide-binding assay. Structure-guided optimization followed and, interestingly, in addition to BCL6 inhibitors, a subset of compounds was identified as BCL6 degraders. BI-3812 acted an as inhibitor, whereas BI-3802 acted as a degrader. Structurally, the authors attributed the different activity to the pyrimidine-R2 substituent; polar or charged moieties resulted in non-degraders, whereas non-polar and lipophilic uncharged moieties resulted in degraders (Fig 4A). Importantly, BI-3802 rapidly induced ubiquitination and degradation of BCL6, resulting in stronger induction of expression of BCL6-repressed genes and significant anti-proliferative effects compared to equipotent non-degradative inhibitors.

In 2020, the cryo-EM structure was reported for BI-3802 and showed that the solvent-exposed moiety of the BCL6 inhibitor contributed to the composite ligand/protein interface.[87] Binding of BI-3802 to the BCL6-BTB domains triggered higher order assembly of BCL6 into filaments. The polymerization resulted in enhanced ubiquitination of BCL6 by the E3 ligase SIAH1, which recognized a VxP motif distal to the binding site. Structurally, the dimethyl piperidine moiety of BI-3802 interacted directly with distal amino acids on the adjacent BTB domain homodimer (Fig 4A). The compound bound in a groove between BCL6 dimers, and the resulting interface resembled the dimer interface observed in the crystal structure. Direct contacts were formed with Tyr58 of BTB α and hydrophobic interactions with Cys84 on the adjacent dimer (BCL6 γ/δ). A key interaction was observed between Arg28 of BTB β and Glu41 of BTB γ, which formed a salt bridge critical for dimer-dimer interaction. The lack of BCL6 polymerization for the structurally similar inhibitor (BI-3812) was attributed to a steric clash of the longer carboxamide group, as indicated by modeling in the cryo-EM structure. An additional systematic alanine scan confirmed that the key resides were located on the polymerization interface (Glu41, Cys84) or in close proximity to the ligand binding site (Gly55, Tyr58).

Also in 2020, Bellenie *et al.*[88] reported a series of benzimidazolone inhibitors of the PPI between BCL6 and its co-repressors. CCT369260, an analog of BI-3802 with improved properties was an orally bioavailable degrader and reduced BCL6 levels in a lymphoma xenograft mouse model. Structurally similar compounds, such as 25a, acted as inhibitors and not degraders. The authors also showed that in the crystal structures of non-degrader 25a and degrader CCT369260 the binding mode was similar and speculated that the nature of the substituents rather than a distinct binding mode might be dictating the degrading or non-degrading behavior of a compound. In contrast to the bulkier carboxamide group in inhibitor BI-3812, for compounds 25a and CCT369260, the size of the substituents was not vastly different. However, a plausible hypothesis was that the oxygen in the morpholine ring (compound 25a, inhibitor) would form polar interactions, whereas the di-fluoro-moiety in that position (CCT369260, degrader) would form non-polar interactions. This observation supports the conclusion reached for BI-3812 and BI-3802.[86]

PD-L1 molecular glues. An interesting case of compounds originally designed as PPI inhibitors, but actually functioning via an entirely different mechanism, are the PD-1/PD-L1 small molecule inhibitors. The PD-1/PD-L1 axis has emerged as a breakthrough target in cancer immunotherapy.[89–91] Programmed death-1 (PD-1), expressed on the surface of activated T lymphocytes, belongs to immune checkpoint receptors. Binding of ligands PD-L1 or PD-L2 induces a co-inhibitory signal in the T-cell. PD-L1 is often overexpressed on the surface of cancer cells and as a result, binding of PD-1 to PD-L1 suppressed antitumor immunity and thus promotes tumor progression.

Following the clinical success of monoclonal antibodies targeting either PD-1 or PD-L1, several classes of small molecules were reported as PD-1/PD-L1 inhibitors.[92–94] Among them was the scaffold originally disclosed by Bristol-Myers Squibb (BMS) in 2015 (*WO2015/034820 A1)*, which included a tri-aromatic core with a mono-ortho substituted biphenyl substructure.[95,96] Representative examples were BMS-8 and BMS-202. Initial biological data were obtained by a homogenous time-resolved fluorescence (HTRF) assay. No further in vitro or in vivo data were disclosed at the time. The true nature of BMS-8 and BMS-202 was

revealed in 2017, when Zak *et al.*[97] reported the crystal structures with human PD-L1 (Fig 4B), supported by several additional biophysical methods, including protein NMR and size exclusion chromatography. The two compounds dissociated the PD-1/PD-L1 complex in NMR studies, induced thermal stabilization of PD-L1, and - as shown in the crystal structures - led to the formation of a compound-PDL1 complex in a ratio of 1:2. Both BMS-8 and BMS-202 bound in a cylindrical, hydrophobic pocket created at the interface of the two monomers. The pocket was solvent accessible on one side of the dimer but restricted by the sidechain of $_{A}$Tyr56 on the opposite side. Both compounds bound in a similar way and formed key interactions with the hot spot amino acids Tyr56, Met115, Ile116, Ala121 and Tyr123 at the dimer interface, forming a stable ternary complex. The 2-methylbiphenyl core was deeply buried in the pocket and formed the majority of interactions with the hot spot residues, including T-stacking interactions with $_{A}$Tyr56, π-alkyl interactions with $_{A}$Met115 and $_{B}$Ala121 and additional hydrophobic interactions. In a subsequent study, the crystal structure of the optimized ligand BMS-1166 was reported[98] (Fig 4B). The homodimerization mechanism was also observed with BMS-1166, a highly potent compound that showed multiple interactions in the dimer interface and caused a rearrangement of Tyr56. The elucidation of the molecular-glue type dimerization mechanism and the unambiguous role of the biphenyl core rapidly enabled the numerous subsequent structure-guided optimization efforts.[99–105]

More recently, it was shown that PD-L1 molecular glues can have distinct effects on degradation pathways. BMS-1166 blocked PD-L1 glycosylation, which is required for the interaction between PD-L1 and PD-1 to occur. Additionally, binding of BMS-1166 to PD-L1 trapped the latter in the endoplasmic reticulum (ER) by preventing the transportation of the newly synthesized PD-L1 into the Golgi, limiting further glycosylation. Consequently, the under-glycosylated PD-L1 in the ER underwent rapid degradation, potentially via the ER-associated protein degradation pathway (ERAD).[106] In contrast to inhibition of protein trafficking, in 2022 Wang *et al.* showed that compound 17, an oxadiazole bis-aryl analog that dimerized PD-L1, promoted the reduction of cell-surface PD-L1 by inducing internalization and lysosomal-dependent degradation of PD-L1.[107] The underlying causes of the opposite degradative effects of PD-L1 molecular glues are not yet fully elucidated.

JH-RE-06 dimerizes REV1. In 2019, Wojtaszek *et al.* described the molecular glue-type mechanism of action of compound JH-RE-06 as an inhibitor of mutagenic translesion DNA synthesis.[108] The compound acted as a dimerization inducer of REV1 and thus a disruptor of the REV1-REV7 PPI. DNA-damaging chemotherapeutics, such as cisplatin, are known to generate DNA lesions, which cannot be repaired by high-fidelity DNA polymerases. To bypass the lesion site at the cost of replication fidelity, specialized DNA polymerases are used in a process known as translesion synthesis (TLS). In mammalian cells, TLS is a two-step process; first, an insertion TLS DNA polymerase (POL η, POL ι, POL κ, and REV1) introduces the nucleotide opposite to the lesion and then an extending TLS DNA polymerase, such as the B-family polymerase complex POL ζ (POL ζ_4: REV3L/REV7/POLD2/POLD3) extends the 3'-terminus. Among these TLS polymerases, REV1 and POL ζ play an important role in the survival of cancer cells in the presence of cisplatin. Therefore, inhibition of REV1-POL ζ interaction is a promising strategy to sensitize cancer cells to chemotherapeutic drugs such as cisplatin and prevent acquisition of drug resistance. However, the development of small molecules inhibitors with high specificity and *in vivo* efficacy has been challenging.

The authors focused on the evolutionarily conserved interaction between REV1 and POL ζ, specifically by targeting a shallow pocket on the REV1 C-terminal domain (CTD) and the REV7 subunit of POL ζ. The authors noted that in addition to the REV7-binding surface to REV1 CTD being shallow, it also contained a conformationally dynamic C-terminal tail, which could further hinder the identification of small molecule inhibitors. An ELISA assay was designed to screen for inhibitors that would specifically target the REV7-binding surface of the REV1 CTD to disrupt the REV1-REV7 interaction. Screening 10,000 structurally diverse compounds led to the identification of compound JH-RE-06, which inhibited the REV1-REV7 interaction at 10 μM. Follow-up validation was performed by a quantitative AlphaScreen assay, revealing an IC_{50} value of 0.78μM, which was in close agreement with the ITC dissociation constant (K_d=0.42μM). ITC showed protein-to-ligand stoichiometry of 2:1 REV1:compound. A co-crystal structure unexpectedly revealed that although the conserved REV7-binding surface of the REV1 CTD was the target of JH-RE-06, the compound bound to the REV1 CTD by inducing its dimerization, consistent with the 2:1 ratio observed by ITC (Fig 5A). Additionally, distinct conformations of the C-terminal tails of the REV1 CTD subunits were observed in the ternary complex, indicating the formation of an asymmetric dimer. Multiple ligand–protein interactions were formed in the dimer interface, including several hydrophobic interactions and direct polar interactions. The formed REV1 CTD dimer created a large binding pocket for JH-RE-06, where nearly all the functional groups of the compound interacted with the monomers. Additionally, the formation of the dimer concealed the REV-7-binding surface, thus blocking the REV1 CTD interaction with REV7 and POL ζ recruitment. Further evaluation of the compound showed that it sensitized tumors to cisplatin and reduced mutagenesis *in vitro*. In xenograft mouse models of human melanomas, co-administration of JH-RE-06 with cisplatin successfully suppressed tumor growth and prolonged animal survival. As the authors highlighted, small molecules could surprisingly target dynamic and seemingly featureless protein interfaces once considered undruggable.

NVS-STG2 oligomerizes STING. In 2023, Li *et al.* reported the activation of human STING (stimulator of interferon genes) by a molecular glue-like compound (NVS-STG2), which induced high-order oligomerization of STING.[109] STING, a dimeric transmembrane adapter protein, has been extensively studied for its role in human innate immune response to infection and for its antitumor activity. High-order oligomerization is required for its activation. Activation occurs by binding of cyclic di-nucleotides (CDNs), such as cGAMP to the ligand-binding domain (LBD) located on the C-terminal cytosolic region of STING. The N-terminal region forms the transmembrane domain (TMD), which includes four transmembrane helices from each subunit that stabilize the dimeric state.

To search for small-molecule activators of STING, HTS phenotypic screening in THP1-dual cells containing an interferon stimulated response element-luciferase (ISRE-Luc) reporter gene was performed. The hit compound NVS-STG1 was characterized by differential scanning fluorimetry (DSF); in contrast to cGAMP, NVS-STG1 did not bind to the LBD of human STING (hSTING). SAR optimization was performed to improve potency before returning to identifying the mechanism of action. The optimized analog NVS-STG2 showed over 100-fold induction of ISRE-Luc reporter and strongly induced phosphorylation of IRF3, the key transcription factor downstream of the STING pathway. Photoaffinity labeling and quantitative chemical

proteomics confirmed that NVS-STG2 had a direct effect on STING. Additionally, the activation of STING by NVS-STG2 was confirmed with an *in vitro* assay by monitoring the high-order oligomerization of purified STING with native gels. In the absence of ligands, STING existed predominantly in a dimeric state. In the presence of cGAMP or C53, a hydrophobic compound that was recently shown to bind in a cryptic pocket in the human TMD,[110] relatively small high-order oligomers were formed. NVS-STG2 strikingly induced high-order oligomerization. The combination of cGAMP, C53, or both with NVS-STG2 promoted the formation of more and larger oligomers, indicating that a different binding site in the TMD was targeted.

Structural biology confirmed and further explained this oligomer-forming mechanism of activation. A cryo-EM structure of STING in complex with cGAMP and NVS-STG2 at 4 Å resolution showed the formation of oligomers consisting of approximately 3-6 dimers. The cryo-EM structure of STING bound to cGAMP/C53/NVS-STG2 at 2.9 Å showed longer and more abundant oligomers, consisting of 10-30 dimers. All three ligands had well-defined densities; two NSV-STG2 molecules bound to the interface between the TMDs of two neighboring STING dimers, while cGAMP bound to the LBD and C53 bound to the TMD pockets within each STING dimer. In both cryo-EM structures, NSV-STG2 effectively acted as a molecular glue that enhanced the interface of two STING dimers and formed stabilizing interactions with both protein surfaces (Fig 5B). The central phenyl group occupied a cavity between the TMDs of the two neighboring STING dimers. The carboxylic acid of NVS-STG2 formed a salt bridge with Arg95 (TM3) and additional electrostatic interactions with Arg94. Additional residues interacting with NVS-STG2 were Gln55, Leu98, Leu134, Leu136 of one STING dimer and Leu134 of the second dimer. Hydrophobic interactions were observed between the ligand and Val48, Leu51, Ala52, Leu101 and Phe105 from one STING dimer and Leu44, Leu47, Leu51 and Leu139 from the second dimer. Notably, more contacts were formed between the TMDs of the two STING dimers, further stabilizing the high-order oligomerization. Overall, the authors rigorously demonstrated the mechanism of action of NVS-STG2 as a molecular glue and provided the structural basis for the rational development of STING agonists or potentially even STING antagonists by introducing bulky compounds that would bind to the pocket without allowing the side-by-side packing required for the high-order oligomerization.

MERS-CoV non-native dimerization. In 2020 Lin *et al.* identified orthosteric stabilizers of a non-native PPI to target the Middle East respiratory syndrome coronavirus (MERS-CoV).[111] This discovery started from a cloning artifact; a non-native dimeric interface was revealed by crystallization of the N-terminal domain of the MERS-CoV nucleocapsid protein (N-NTD), in contrast to previous N-NTD monomeric structures. The dimerization was facilitated by two nonendogenous N-terminal vector-fusion residues (His37 and Met38) that were present during protein expression. Cross-linking experiments and further analysis of the dimeric structure showed that residue Trp43 was essential for the formation of the hydrophobic pocket that accommodated the vector-fusion residues and mediated the dimerization. A structure-based virtual screen was performed, targeting the hot spot residue Trp43. The hits were filtered based on shape and hydrophobic complementarity and three compounds were selected for further evaluation. One of them, 5-benzyloxygramine (P3) was able to stabilize wildtype MERS-CoV N-NTD via fluorescent thermal stability assays. A crystal structure of compound P3 with full length wildtype MERS-CoV N-NTD showed the N-NTD as a dimer, with compound P3 forming multiple hydrophobic interactions with both monomers (Fig 5C).

Small-angle X-ray scattering (SAXS) and cell-based assays further revealed that compound P3 induced abnormal full-length N protein oligomerization, decreased MERS-CoV nucleocapsid protein and suppressed N protein expression. The compound halted both viral production and replication in Vero6 cells after 48 h at 100 μM.

ISRIB acts as a "molecular staple" stabilizing the active decameric form of the eIF2B holoenzyme. The eukaryotic integrated stress response (ISR) senses and integrates diverse stressors. ISR reprograms translation and controls protein homeostasis, providing a checkpoint for cells to repair damage or induce cell death. The ISR is controlled by phosphorylation of the general eukaryotic translation initiator factor eIF2. Four upstream kinases (PERK, PKP, GCN2, HRI) are activated by different stress conditions. In turn, they phosphorylate Ser51 in the α-subunit of eIF2 (eIF2α). eIF2 binds GTP and the initiator Met-tRNA to form the ternary complex (eIF2-GTP-Met-tRNAi), which then associates with the 40S ribosomal subunit to form the 43S pre-initiator complex (PIC) that scans the 5'UTR of mRNAs for the initiating AUG codons. Phosphorylation of Ser51 in eIF2α turns eIF2 into a competitive inhibitor of its guanine exchange factor (GEF), eIF2B. The binding of phosphorylated eIF2 to eIFB2 prevents the interaction of the eIF2 complex with GTP. Thus, when Ser51 is phosphorylated, formation of the ternary complex is blocked, and translation initiation is reduced. The difference in the relative abundance of eIF2B and eIF2 indicates that phosphorylation of even a small fraction of the total eIF2 will have a significant cellular effect. While phosphorylation diminishes general protein synthesis, it allows the preferential translation of some mRNAs that contain upstream open reading frames (uORFs) in their 5'UTR.

In 2013, Sidrauski *et al*.[112] performed a cell-based screen for inhibitors of PERK signaling, which lies at the intersection of ISR and the unfolded protein response (UPR) that maintains protein homeostasis in ER. The authors screened a library of ~107K compounds using an engineered luciferase reporter assay that allowed monitoring of PERK activation in living cells. Hits were triaged using an orthogonal assay that employed a fluorescent reporter and microscopy read-out; twenty-eight compounds were validated. One of the validated hits, a symmetric compound called ISRIB (integrated stress response inhibitor), was highly potent at blocking the ISR in cells (IC_{50} = 40 nM). The two diastereomers were synthesized and the *trans*-ISRIB was 100-fold more potent than *cis*-ISRIB (IC_{50} = 5 nM and 600 nM, respectively). Further validation of ISRIB showed that ISRIB did not affect PERK phosphorylation or kinase activity. Instead, cells treated with ISRIB were resistant to the effects of eIF2α phosphorylation at Ser51. ISRIB had favorable pharmacokinetic properties, crossed the blood-brain barrier, and was further evaluated in rodents, where it enhanced cognitive function and increased long-term memory. The overall effects of ISRIB suggested that eIF2α phosphorylation played a significant role in the modulation of higher-order brain function; however, the molecular target of ISRIB was unknown.

Shortly after the identification of ISRIB, two structural papers demonstrated that eIF2B was a heterodecameric complex.[113,114] In 2015, two independent groups almost simultaneously reported mechanistic studies that revealed that eIF2B was the molecular target of ISRIB. Sidrauski *et al.,*[115] using unbiased genetic screens and structure/activity analyses, showed that ISRIB was an activator of eIF2B, induced the self-association of eIF2B in cells, and enhanced the GEF activity of eIF2B. The symmetry of the

molecule was crucial for the stabilization of the activated eIF2B in cells, as supported by further SAR. Sekine *et al.*[116] explored ISRIB's mechanism of action by screening cultured mammalian cells for somatic mutations that reversed the effect of ISRIB on the ISR. This study showed that ISRIB targeted an interaction between eIF2 and eIF2B and functioned independently of eIF2 phosphorylation. In 2016, Hearn *et al.*[117] described thorough structure-activity relationships of ISRIB analogs. The improved analogs, with picomolar cellular IC_{50} values, made cells insensitive to the effects of eIF2α phosphorylation by activating eIF2B and allowing global protein synthesis to proceed with residual unphosphorylated eIF2α. The authors hypothesized that the compounds stabilized the formation of the eIF2B protein complex.

Proof of the binding mode of ISRIB came in 2018, when Tsai *et al.* reported the cryo-EM structure[118] (Fig 5D). Formation of the fully active, decameric human eIF2B holoenzyme depended on the assembly of two identical tetrameric subcomplexes, followed association of the eIF2Bα homodimer. ISRIB bound in a deep cleft within this decameric eIF2B at the central symmetry interface. Structurally, residues in the N-terminal loop of the δ subunit contributed significantly to the binding of ISRIB (δVal177, δLeu179, δLeu485) with hydrophobic interactions. The center of the binding site was formed by residues in the β subunit (βAsn162, βHis188) that were closer to the more polar moieties of ISRIB, whereas hydrophobic residues were also involved (βVal164, βIle190). A key interaction was the C-H-π interaction between one of the two C-H bonds of the glycolamide α-carbon of ISRIB and the aromatic histidine ring of βHis188; mutation of His to Ala led to loss of stabilization of the decamer by ISRIB. Notably, ISRIB did not form direct interactions with the α subunit, but instead stabilized the symmetry interface of the β- and δ- subunits, which enhanced the stable binding of the eIF2B(α_2).

Two additional cryo-EM studies were published in 2020[119] and 2021[120] focusing on allostery. Zyryanova *et al.*[119] showed that ISRIB and the Ser51-phosphorylated eIF2α [eIF2(αP)], bound distinct sites in their common target, eIF2B. Nevertheless, *in vitro*, ISRIB and eIF2(αP) reciprocally opposed each other's binding to eIF2B. Cryo-EM also showed that binding of both eIF2B regulatory sites by two eIF2(αP) molecules remodeled both the ISRIB-pocket and the pockets that would engage eIF2α during active nucleotide exchange; thus, both binding events cannot occur simultaneously. These observations demonstrated that ISRIB and eIF2(αP) were mutually incompatible ligands of eIF2B, indicating the significance of antagonistic allostery. In 2021, Schoof *et al.*[120] additionally showed that ISRIB promoted the assembly of eIF2B tetramers into active octamers and also inhibited the ISR even when eIF2B decamers were fully assembled. Cryo-EM structures supported the allosteric communication of physically distant eIF2, phosphorylated eIF2, and ISRIB binding sites. The overall evolution of the understanding of ISRIB's mechanism of action indicated that although it was initially considered an inhibitor of the ISR, it had stabilizing PPI properties, that would allow its classification as a "molecular staple."

All these examples of self-association were selected as representative cases of compound-induced effects. However, it is worth mentioning that this might not always be the real cause of high-order protein polymerization and thus investigating the underlying mechanisms is crucial. One unusual example that falls in the latter category was reported by Morreale et al.[121] The authors identified a fragment targeting the Fanconi anemia ubiquitin-conjugating enzyme Ube2T. Although biophysical and biochemical

characterization supported the observed activity, the co-crystal structure indicated that the observed effects were in fact caused by a contaminating zinc ion. Surprisingly, zinc binding to the active site cysteine induced an unprecedented domain swap in Ube2T that resulted in target trimerization. Whether this was a unique case for metal ions, or a small molecule might be able to induce a domain swap remains to be seen. Nevertheless, orthogonal assays and structural information are fundamental for deciphering the causes of compound induced self-association.

Discussion

The dramatic entry of molecular glues on the drug-discovery scene has fundamentally changed our understanding of how to modulate PPIs. Targets once considered undruggable via traditional strategies have been successfully targeted with MGs. Since MGs can target both native and neomorphic PPIs, there are now vast opportunities to modulate PPIs in ways that a decade ago were inconceivable. New concepts, such as shape complementarity at the PPI interface, cooperativity, and compound-induced proximity, had to be developed to characterize MGs and are now allowing drug hunters to identify them in a more rational way. Better understanding of both the structure and dynamics of PPI interfaces – thanks in large part to cryo-EM – have been pivotal to enhancing our understanding of how MGs work on an atomic level. In particular, MGs bind to both sides of a protein interface and induce or enhance formation of the PPI itself; both MG/protein and protein-protein interactions define a highly cooperative complex.

When MGs like CELMoDs were first characterized, the PPIs were not thought to exist without the MGs and were thus “neomorphic” interactions. By contrast, natural products like fusicoccanes stabilized existing interactions. Further structural and functional analysis suggests that these two ideas exist on a continuum. For instance, there is often an intrinsic affinity and shape complementary between the proteins, such as the DDB1-CDK12 example, that is too weak to have a biological effect, but that is stabilized by the MG which “glues the complementary surfaces” by forming interactions with hotspot residues at the interface. Thus, the MG converts a weak affinity PPI to a highly cooperative ternary complex. Thermodynamic modeling[57] provides a framework to quantify the different binding interactions and to calculate the intrinsic cooperativity for the ternary (or larger) complex. The incorporation of “omic” approaches and large-scale datasets have also revolutionized the field by facilitating deconvolution of phenotypic screens and the identification of molecular targets. The huge structural diversity of PPIs provides countless opportunities both for chemical biology and drug discovery.

As shown in the examples here, diverse strategies can be employed to discover MGs rationally. Some approaches include:

Cell-based screens. Traditionally, phenotypic screens have led to the discovery of first-in-class drugs, whereas target-based approaches have led to more best-in-class drugs.[122] While phenotypic screens yield cell active compounds directly, defining the molecular target can be complex. In the case of MGs, several companies have screened MG-like libraries in cells and monitored degradation of a target-of-interest. This approach limits the target deconvolution scope to validating the degradation mechanism. As shown in the

case of cyclin K degraders, diverse phenotypic screen approaches can be highly successful in the identification of MGDs.

Biophysical assays adapted to stabilization. Typically, target-based screens in the MG space use proximity assays, such as fluorescence polarization/anisotropy or energy transfer, that monitor the formation of the PPI. When using these assay formats to screen for inhibitors, usually only the EC_{50} – the concentration of compound at which 50% of the PPI is inhibited – needs to be measured. For stabilization assays, however, one must evaluate two independent parameters – the EC_{50} and the quantification of efficacy/cooperativity. This would include the quantification of fold-stabilization, ie, the shift in *app*K_d from native binary complex to ternary complex in the presence of the MG[52,74,82]. Depending on the complexity of the system, α factor determination and thermodynamic modeling could also be applied.[57] Screening for a gain-of-function instead of inhibition in a biophysical setting requires modification of screening conditions. Typically, FP/TR-FRET screens are performed at EC_{20}. As the efficiency of MGs improves, it is not uncommon to encounter affinities tighter than the theoretical dynamic range of the assay. To circumvent this issue modifications in the concentrations of reagents are necessary. The associated challenge, however, is the limited assay window. In certain cases, biophysical assays rely on the use of peptides to simplify the screens. Caution is required to ensure that the simplification of the system does not overly compromise its biological relevance or artificially reduce the opportunity to identify a MG; for instance, ZBTB16 has nine Zn-finger domains and so far, two of them that can be induced to bind CRBN with different MGs.[36] In general, humility must accompany biochemical and biophysical assays, since for the sake of precision, we simplify the system and likely sacrifice some biological context. The mechanistic picture emerges through a diversity of assay formats, including diverse cellular readouts.

Covalent MGs. Another challenge for MG discovery is the 3-body problem, especially in systems with low intrinsic affinity and/or when one of the targets is intrinsically disordered. The 3-body problem refers to the need for both proteins and the molecule to associate at the same time, which is statistically unlikely. In the case of IMiDs/CeLMODs, the MGDs have high affinity for CRBN; however, in the general case, the MG could bind weakly to both partners yet with high cooperativity to the PPI complex. In this case, reversible or irreversible covalent modes of screening are particularly well-suited, since covalency enhances the affinity to one of the proteins and could slow the binding kinetics to approximate a 2-body association. Covalent screening approaches include chemoproteomics with irreversible binders[123,124] and biophysical screens with irreversible or reversible binders.[72,73,80] Reversible covalent ligands, such as the aldehydes and disulfides screened for 14-3-3, have the further advantage that binding is thermodynamically (vs kinetically) driven. Thus, compounds are identified as MGs because the ternary complex is most stable, rather than just the fastest to form.

Needless to say, there is a lot of excitement for the discovery of MGs and the term is encountered more and more often in recent publications. We believe, however, that this term should not be used lightly. Instead, it should be demonstrated that compounds act as MGs. First, the formation of a ternary complex in the presence of the glue should be exemplified, ideally with a structure, but also using biophysical methods, cell-based assays, and/or mutagenesis. Another key factor for defining a MG would be the

evidence of cooperativity at the PPI interface, since MGs show weak or low affinity to at least one of the binding proteins. For bifunctional molecules, such as PROTACs, cooperativity is not strictly required, as in some cases PROTACs with negative cooperativity were still able to lead to target degradation.

What do we expect to see 10 years from now?

As the field of MGs is rapidly evolving, we have great expectations for the next 10 years. A distinction is appropriate here between MGDs and the other subtypes of MGs, since MGDs are the main type currently evaluated in clinical trials. This primarily includes MGDs targeting CRBN and E7820 that targets DCAF15. An overview of current status of clinical trials can be found in recent reviews. [125,126]

For MGDs, we expect extensive research efforts targeting new ligases, identifying diverse neosubstrates, and new degrons. Chemical biology tools can significantly aid our understanding of the mechanism of action of molecular glues. In recent reports there is the emerging concept that MGDs often stabilize pre-existing, E3 ligase/target interactions, which might functionally appear to be inconsequential in the absence of the glue.[6,127,128] Weak, nonfunctional interactions suggest a continuum between 'native PPI' and 'neomorphic PPI' that can be stabilized by a MG.

New mechanisms and strategies for targeted degradation are actively being pursued at multiple biotech companies, and there are already published examples moving in this direction. For instance, the PI3K inhibitor inavolisib/GDC-0077 was recently reported to act as degrader of mutant PI3Kα. The exact mechanism of degradation remains unclear for now.[129] Interesting approaches have been described recently for the development of BRD4 degraders, starting from the structure of the well-known BET bromodomain inhibitor, JQ1 (Fig 6A). The solvent exposed moiety bearing a p-Cl substituent was modified to include an alkynyl "degradation tail", resulting in monovalent BRD4 degraders, including compound GNE-0011.[130,131] A CRISPR screen revealed that this BRD2/4 MGD recruited DCAF16.[132] Although the structural and biochemical characterization were pending, the recruitment of the relatively uncharacterized E3 ligase DCAF16 was intriguing. Earlier this year, a series of covalent BRD4 MGDs that bind to DCAF16 were reported.[133] These compounds were derivatives of JQ1 and contained diverse electrophilic warheads. The cryo-EM of the ternary complex of compound MMH2 with DCAF16 and $BRD4^{BD2}$ was reported and interestingly supports the notion of pre-existing structural complementarity between DCAF16 and BRD4 (Fig 6B). The solvent-exposed covalent warhead on the BRD4 inhibitor recruited the E3 ligase by binding to Cys58 on DCAF16. In contrast to non-covalent MGs, in this case the hook effect was observed. The authors also noted that DCAF16, unlike most other DCAF proteins, lacked the canonical WD40 propeller and was predicted to be largely unstructured. This ligase-as-intrinsically-disordered-protein represented a more extreme case for the structural adaptivity already seen for CRBN[40], which was found to have a high degree of conformational flexibility that might facilitate the glue-type activity. Further studies should explore the role of protein dynamics in our ability to discover MGDs.

An intriguing new mechanism of action was reported by Ciulli *et al.* regarding intramolecular bivalent glues (IBGs).[128]Although our main focus on this review was on monovalent molecular glues, this very recent work described a "new modality" that lay in the gray zone between monovalent glues and bivalent

degraders. Compound IBG1 comprised the BET bromodomain inhibitor JQ1 and the aryl sulfonamide E7820 (the MGD of RBM39 that recruited DCAF15; Fig 1B). In contrast to a typical PROTAC mechanism of action, IBG1 degraded BRD4 by binding intramolecularly in two adjacent domains on BRD4 (BD1 and BD2) and inducing a conformational change, which was recognized by the E3 ligase DCAF16, not DCAF15. Orthogonal biophysical assays, including ITC, TR-FRET, AlphaLISA displacement assays and SEC proved the intrinsic basal affinity between BRD4 and DCAF16, which was enhanced by IBG1 in the presence of both bromodomains. A cryo-EM structure of the ternary complex of IBG1/BRD4/DCAF16/DDB1 showed that both bromodomains (BD1, BD2) bound simultaneously to DCAF16. IBG1 bound at the interface of DCAF16/BD1/BD2 with its JQ1 portion in the BD2 pocket and the E7820 portion in the BD1 pocket (Fig 6C). This binding mode significantly enhanced the surface complementarity with the E3 ligase. The authors also showed that a structurally similar compound, IBG4, comprising of JQ1 and a short rigid ligand, degraded BRD4 via DCAF11. In both cases, intrinsic affinities were identified between BRD4 and the E3 ligases in the absence of the compounds, supporting the emerging concept of pre-existing interactions between E3 ligases and target proteins.

The generalizability of bifunctional degraders, eg, PROTACs, has led to a burst of creative induced-proximity designs. As examples, diverse bifunctional molecules have been demonstrated to functionally activate deubiquitinases, kinases, phosphatases, and acetyl transferases towards proteins-of-interest and RNA nucleases towards RNAs-of-interest (comprehensively reviewed in [9]). In principle, MGs could also perform these mechanisms of action, if suitable discovery assays could be developed. As with MGs discovered to date, such compounds could activate native complexes or induce non-native biology.

For rationally designed, non-degradative molecular glues and glues inducing self-association, it remains to be seen how rewiring of the underlying biology and PPI modulation translates into a clinical outcome. A potentially groundbreaking non-degradative MG was recently reported for KRAS[134], including chemical remodeling of a cellular chaperone (CYPA). A natural product-inspired macrocycle remodels the surface of cyclophilin A, creating a neomorphic interface that has high affinity and selectivity for the active state of mutant $KRAS^{G12C}$. Notably, neither CYPA nor its natural product ligand were previously reported to interact with KRAS. The resulting tricomplex inactivated oncogenic signaling. An optimized ligand is currently undergoing clinical trials.

Overall, for all types of MGs we anticipate that chemical biology approaches will further elucidate aspects of molecular recognition, shape complementarity, cooperativity, underlying dynamics, and degrons for E3 ligases. For instance, observations of a very narrow SAR or observed SAR for seemingly solvent exposed parts of the molecule in binary crystal structures could be hints that one should look for a glue-like mechanism of action. As shown here with multiple examples, the solvent-exposed parts of the molecules, although typically considered of minor importance, were actually fundamental for molecular recognition and the glue-like mechanism of action. Representative examples were the CELMoDs, the degraders of cyclin K, the BCL6 degraders, the PD-L1 MGs and the BRD4 MGDs. Eventually, we anticipate that one will be able to predict the ternary complexes formed based on the composite surface of the protein+glue. Furthermore, we expect to see many more MGs, now that investigators are more likely to systematically

distinguish inhibitors from glues early in compound validation. The better understanding of chemical biology will largely enable the more rational and efficient development of new clinical tools. Vice versa, data from on-going clinical trials will allow better understanding of potential limitations of the field, including the identification of the most appropriate proteins to target.

ACKNOWLEDGEMENTS: We would like to thank Phil Chamberlain for insightful discussions, and our lab collaborators Luc Brunsveld and Christian Ottmann for inspiration. Funding was received from NIH/NIGMS GM147696 and Ono Pharma Foundation Breakthrough Science Initiative Award. Figures were prepared with Biorender (TOC), Adobe Illustrator 2024, Pymol (version 4.6.0) and ChemDraw (version 22.0.0)

DECLARATION OF INTERESTS: The authors declare the following competing financial interests. M.R.A is a co-founder and consultant of Ambagon Therapeutics.

Figure and table legends

Figure 1. **Molecular glue degraders for $CRL4^{CRBN}$ and $CRL4^{DCAF15}$**

A. Ternary complexes of CELMoD compounds, interacting aminoacids and chemical structures. Top left: crystal structure of lenalidomide/CRBN/DDB1 (PDB 4TZ4). Top middle: crystal structure of lenalidomide/CRBN/DDB1/CK1α (PDB 5FQD). Top right: crystal structure of CC-885/CRBN/DDB1/GSPT1 (PDB 5HXB). Bottom left: crystal structure of CC-220 (iberdomide)/CRBN/DDB1 (PDB 5V3O). Bottom middle: crystal structure of CC-90009 (eragidomide)/CRBN/DDB1/GSPT1 (PDB 6XK9). Bottom right: cryo-EM structure of CC-92480 (mezigdomide)/CRBN/DDB1/Ikaros ZF1-2-3 (PDB 8D7Z). B. Left: cryo-EM structure of human DDB1-DDA1-DCAF15 E3 ubiquitin ligase bound to RBM39 and indisulam (PDB 6SJ7). Middle: close-up views on interacting amino acids with MGD indisulam (PDB 6SJ7), tasisulam (PDB 6Q0V) and E7820 (PDB 6Q0R). Right: chemical structures of RBM39 MGDs.

Figure 2. **Molecular glue degraders of cyclin K and β-catenin**

A. Top feft: the cyclin K/CDK12/DDB1 complex with a molecular glue degrader (PDB 6TD3). Top right: structural diversity of cyclin K MGDs, middle: ternary complexes with MGDs/CDK12/DDB1 and interacting aminoacids (PDBs 6TD3, 8BUC, 8BUB, 8BUG, 8BU5, 8BUH, 8BU7, 8BUA). B. Left: Monophosphorylated pSer33 β-Catenin peptide bound to b-TrCP/Skp1 complex (PDB 6M94), middle: ternary complexes with MGDs/monophosphorylated pSer33 β-Catenin peptide/ b-TrCP/Skp1 (PDBs 6M93, 6M92, 6M91), right: chemical structures of β-catenin MGDs.

Figure 3. Non-degradative molecular glues / PPI stabilizers for 14-3-3/clients, KSR/MEK and GLP-1R/GLP-1

A. Ternary complexes of 14-3-3/client PPI stabilizers, chemical structures, and close-up view of interactions; top right: compound 3/14-3-3/ChREPB (PDB 6YGJ), middle right: compound 23/14-3-3/PIN1 (PDB 7BG3), bottom left: fragment 7/14-3-3/CRAF (PDB 8A6H), bottom middle: non-covalent compound 24/14-3-3/ERα (PDB 8BWX), bottom right: covalent compound 181/14-3-3/ERα (PDB 8APS). B. Cooperativity model to quantify the efficacy of 14-3-3/client PPI stabilizers. C. Crystal structure of ternary complex MG/MEK/KSR2. Chemical structures of trametinib and trametiglue and close-up view of interacting amino acids (PDB 7JUR and 7JUV, respectively). D. Cryo-EM structure of the GLP-1R complex bound to LSN3160440 with full-length GLP-1, heterotrimeric G_s and the camelid antibody Nb35 (PDB 6VCB), close-up view and chemical structure of LSN3160440.

Figure 4. **Molecular glues inducing self-association: BCL6 degraders and PD-L1 molecular glues**

A. Left: Chemical structures of BCL6 inhibitors and molecular glues. Top middle: crystal structure of MG BI-3802 in BCL6 BTB domain (PDB 5MW2), and cryo-EM structure of BI-3802 in the polymer BCL6 (PDB 6XMX), with a close-up view of interacting amino acids at the interface. Top right: crystal structure of inhibitor compound 25a in BCL6 BTB domain (PDB 6TOL). Bottom right: crystal structure of MG CCT369260 in BCL6 BTB domain (PDB 6TOM). B. Left: Ligand-induced dimerization of PD-L1. Examples of chemical structures and crystal structures of PD-L1 ligand-bound dimers with a close-up view of interacting amino acids.

Figure 5. **Molecular glues inducing self-association: REV1, STING, MERS-CoV and eIF-2B**

A. Left: Chemical structure of JH-RE-06. Middle: two REV1 monomers with the ligand bound in the dimeric interface. Right: close-up view of interacting amino acids (PDB 6C8C). B. Left: chemical structure of NVS-STG2. Middle: cryo-EM structure of STING bound to cGAMP (cyan sticks) and NVS-STG2 (magenta), and close-up of interacting amino acids (PDB 8FLK). Right: Cryo-EM structure of STING bound to cGAMP (cyan sticks), NVS-STG2 (magenta) and C53 (purple spheres), and close-up with interacting amino acids (PDB 8FLM). C. Left: chemical structure of 5-benzyloxygramine (P3). Middle: crystal structure of the dimer MERS-CoV N-NTD with the ligand bound in the dimeric interface. Right: close-up view of interacting amino acids at the interface (PDB 6KL6). D. Left: chemical structure of ISRIB. Middle:

cryo-EM decameric structure with ISRIB bound at the interface of subunits beta/delta. Right: close-up view of interacting amino acids at the interface (PDB 7L7G).

Figure 6. BRD4 inhibitors and molecular glues

A. Chemical structures of a BRD4 inhibitor, monovalent MGDs and intramolecular bivalent glues (IBGs). B. Left: Chemical structure of MMH2. Middle: cryo-EM structure of MMH2 bound to DDA1/DDB1/DCAF16/BRD4^{BD2}. Right: close-up view of interacting amino acids (PDB 8G46). C. Left: chemical structure of IBG1. Middle: cryo-EM structure of IBG1 bound to DDB1deltaBPB/DCAF16/BRD4$^{BD1/BD2}$. Right: close-up view of interacting amino acids (PDB 8OV6).

Table S1. Overview of molecular glues, classification, and main experimental techniques

REFERENCES

1. Arkin, M.R., and Wells, J.A. (2004). Small-molecule inhibitors of protein–protein interactions: progressing towards the dream. Nat Rev Drug Discov *3*, 301–317. 10.1038/nrd1343.

2. Arkin, M.R., Tang, Y., and Wells, J.A. (2014). Small-Molecule Inhibitors of Protein-Protein Interactions: Progressing toward the Reality. Chemistry & Biology *21*, 1102–1114. 10.1016/j.chembiol.2014.09.001.

3. Domostegui, A., Nieto-Barrado, L., Perez-Lopez, C., and Mayor-Ruiz, C. (2022). Chasing molecular glue degraders: screening approaches. Chem. Soc. Rev. *51*, 5498–5517. 10.1039/D2CS00197G.

4. Kozicka, Z., and Thomä, N.H. (2021). Haven't got a glue: Protein surface variation for the design of molecular glue degraders. Cell Chemical Biology *28*, 1032–1047. 10.1016/j.chembiol.2021.04.009.

5. Schreiber, S.L. (2021). The Rise of Molecular Glues. Cell *184*, 3–9. 10.1016/j.cell.2020.12.020.

6. Rui, H., Ashton, K.S., Min, J., Wang, C., and Potts, P.R. (2023). Protein–protein interfaces in molecular glue-induced ternary complexes: classification, characterization, and prediction. RSC Chem. Biol. *4*, 192–215. 10.1039/D2CB00207H.

7. Sakamoto, K.M., Kim, K.B., Kumagai, A., Mercurio, F., Crews, C.M., and Deshaies, R.J. (2001). Protacs: chimeric molecules that target proteins to the Skp1-Cullin-F box complex for ubiquitination and degradation. Proc Natl Acad Sci U S A *98*, 8554–8559. 10.1073/pnas.141230798.

8. Ng, C.S.C., and Banik, S.M. (2022). Recent advances in induced proximity modalities. Current Opinion in Chemical Biology *67*, 102107. 10.1016/j.cbpa.2021.102107.

9. Liu, X., and Ciulli, A. (2023). Proximity-Based Modalities for Biology and Medicine. ACS Cent. Sci. *9*, 1269–1284. 10.1021/acscentsci.3c00395.

10. Békés, M., Langley, D.R., and Crews, C.M. (2022). PROTAC targeted protein degraders: the past is prologue. Nat Rev Drug Discov *21*, 181–200. 10.1038/s41573-021-00371-6.

11. Gadd, M.S., Testa, A., Lucas, X., Chan, K.-H., Chen, W., Lamont, D.J., Zengerle, M., and Ciulli, A. (2017). Structural basis of PROTAC cooperative recognition for selective protein degradation. Nat Chem Biol *13*, 514–521. 10.1038/nchembio.2329.

12. Lai, A.C., and Crews, C.M. (2017). Induced protein degradation: an emerging drug discovery paradigm. Nat Rev Drug Discov *16*, 101–114. 10.1038/nrd.2016.211.

13. Wurz, R.P., Rui, H., Dellamaggiore, K., Ghimire-Rijal, S., Choi, K., Smither, K., Amegadzie, A., Chen, N., Li, X., Banerjee, A., et al. (2023). Affinity and cooperativity modulate ternary complex formation to drive targeted protein degradation. Nat Commun *14*, 4177. 10.1038/s41467-023-39904-5.

14. Zorba, A., Nguyen, C., Xu, Y., Starr, J., Borzilleri, K., Smith, J., Zhu, H., Farley, K.A., Ding, W., Schiemer, J., et al. (2018). Delineating the role of cooperativity in the design of potent PROTACs for BTK. Proc. Natl. Acad. Sci. U.S.A. *115*. 10.1073/pnas.1803662115.

15. Schiemer, J., Horst, R., Meng, Y., Montgomery, J.I., Xu, Y., Feng, X., Borzilleri, K., Uccello, D.P., Leverett, C., Brown, S., et al. (2021). Snapshots and ensembles of BTK and cIAP1 protein degrader ternary complexes. Nat Chem Biol *17*, 152–160. 10.1038/s41589-020-00686-2.

16. Nowak, R.P., DeAngelo, S.L., Buckley, D., He, Z., Donovan, K.A., An, J., Safaee, N., Jedrychowski, M.P., Ponthier, C.M., Ishoey, M., et al. (2018). Plasticity in binding confers selectivity in ligand-induced protein degradation. Nat Chem Biol *14*, 706–714. 10.1038/s41589-018-0055-y.

17. Gray, W.M., Kepinski, S., Rouse, D., Leyser, O., and Estelle, M. (2001). Auxin regulates SCFTIR1-dependent degradation of AUX/IAA proteins. Nature *414*, 271–276. 10.1038/35104500.

18. Tan, X., Calderon-Villalobos, L.I.A., Sharon, M., Zheng, C., Robinson, C.V., Estelle, M., and Zheng, N. (2007). Mechanism of auxin perception by the TIR1 ubiquitin ligase. Nature *446*, 640–645. 10.1038/nature05731.

19. Sheard, L.B., Tan, X., Mao, H., Withers, J., Ben-Nissan, G., Hinds, T.R., Kobayashi, Y., Hsu, F.-F., Sharon, M., Browse, J., et al. (2010). Jasmonate perception by inositol-phosphate-potentiated COI1–JAZ co-receptor. Nature *468*, 400–405. 10.1038/nature09430.

20. Isobe, Y., Okumura, M., McGregor, L.M., Brittain, S.M., Jones, M.D., Liang, X., White, R., Forrester, W., McKenna, J.M., Tallarico, J.A., et al. (2020). Manumycin polyketides act as molecular glues between UBR7 and P53. Nat Chem Biol *16*, 1189–1198. 10.1038/s41589-020-0557-2.

21. Ito, T., Ando, H., Suzuki, T., Ogura, T., Hotta, K., Imamura, Y., Yamaguchi, Y., and Handa, H. (2010). Identification of a Primary Target of Thalidomide Teratogenicity. Science *327*, 1345–1350. 10.1126/science.1177319.

22. Vargesson, N. (2015). Thalidomide-induced teratogenesis: History and mechanisms. Birth Defects Research Pt C *105*, 140–156. 10.1002/bdrc.21096.

23. Chamberlain, P.P., Lopez-Girona, A., Miller, K., Carmel, G., Pagarigan, B., Chie-Leon, B., Rychak, E., Corral, L.G., Ren, Y.J., Wang, M., et al. (2014). Structure of the human Cereblon–DDB1–lenalidomide complex reveals basis for responsiveness to thalidomide analogs. Nat Struct Mol Biol *21*, 803–809. 10.1038/nsmb.2874.

24. Fischer, E.S., Böhm, K., Lydeard, J.R., Yang, H., Stadler, M.B., Cavadini, S., Nagel, J., Serluca, F., Acker, V., Lingaraju, G.M., et al. (2014). Structure of the DDB1–CRBN E3 ubiquitin ligase in complex with thalidomide. Nature *512*, 49–53. 10.1038/nature13527.

25. Gandhi, A.K., Kang, J., Havens, C.G., Conklin, T., Ning, Y., Wu, L., Ito, T., Ando, H., Waldman, M.F., Thakurta, A., et al. (2014). Immunomodulatory agents lenalidomide and pomalidomide co-stimulate T cells by inducing degradation of T cell repressors I karos and A iolos via modulation of the E 3 ubiquitin ligase complex CRL 4 ^{CRBN} . Br J Haematol *164*, 811–821. 10.1111/bjh.12708.

26. Krönke, J., Udeshi, N.D., Narla, A., Grauman, P., Hurst, S.N., McConkey, M., Svinkina, T., Heckl, D., Comer, E., Li, X., et al. (2014). Lenalidomide Causes Selective Degradation of IKZF1 and IKZF3 in Multiple Myeloma Cells. Science *343*, 301–305. 10.1126/science.1244851.

27. Lu, G., Middleton, R.E., Sun, H., Naniong, M., Ott, C.J., Mitsiades, C.S., Wong, K.-K., Bradner, J.E., and Kaelin, W.G. (2014). The Myeloma Drug Lenalidomide Promotes the Cereblon-Dependent Destruction of Ikaros Proteins. Science *343*, 305–309. 10.1126/science.1244917.

28. Krönke, J., Fink, E.C., Hollenbach, P.W., MacBeth, K.J., Hurst, S.N., Udeshi, N.D., Chamberlain, P.P., Mani, D.R., Man, H.W., Gandhi, A.K., et al. (2015). Lenalidomide induces ubiquitination and degradation of CK1α in del(5q) MDS. Nature *523*, 183–188. 10.1038/nature14610.

29. Petzold, G., Fischer, E.S., and Thomä, N.H. (2016). Structural basis of lenalidomide-induced CK1α degradation by the CRL4CRBN ubiquitin ligase. Nature *532*, 127–130. 10.1038/nature16979.

30. Matyskiela, M.E., Lu, G., Ito, T., Pagarigan, B., Lu, C.-C., Miller, K., Fang, W., Wang, N.-Y., Nguyen, D., Houston, J., et al. (2016). A novel cereblon modulator recruits GSPT1 to the CRL4(CRBN) ubiquitin ligase. Nature *535*, 252–257. 10.1038/nature18611.

31. Matyskiela, M.E., Zhang, W., Man, H.-W., Muller, G., Khambatta, G., Baculi, F., Hickman, M., LeBrun, L., Pagarigan, B., Carmel, G., et al. (2018). A Cereblon Modulator (CC-220) with Improved Degradation of Ikaros and Aiolos. J. Med. Chem. *61*, 535–542. 10.1021/acs.jmedchem.6b01921.

32. Donovan, K.A., An, J., Nowak, R.P., Yuan, J.C., Fink, E.C., Berry, B.C., Ebert, B.L., and Fischer, E.S. (2018). Thalidomide promotes degradation of SALL4, a transcription factor implicated in Duane Radial Ray syndrome. eLife *7*, e38430. 10.7554/eLife.38430.

33. Sievers, Q.L., Petzold, G., Bunker, R.D., Renneville, A., Słabicki, M., Liddicoat, B.J., Abdulrahman, W., Mikkelsen, T., Ebert, B.L., and Thomä, N.H. (2018). Defining the human C2H2 zinc finger degrome targeted by thalidomide analogs through CRBN. Science *362*, eaat0572. 10.1126/science.aat0572.

34. Furihata, H., Yamanaka, S., Honda, T., Miyauchi, Y., Asano, A., Shibata, N., Tanokura, M., Sawasaki, T., and Miyakawa, T. (2020). Structural bases of IMiD selectivity that emerges by 5-hydroxythalidomide. Nat Commun *11*, 4578. 10.1038/s41467-020-18488-4.

35. Matyskiela, M.E., Clayton, T., Zheng, X., Mayne, C., Tran, E., Carpenter, A., Pagarigan, B., McDonald, J., Rolfe, M., Hamann, L.G., et al. (2020). Crystal structure of the SALL4–pomalidomide–cereblon–DDB1 complex. Nat Struct Mol Biol *27*, 319–322. 10.1038/s41594-020-0405-9.

36. Matyskiela, M.E., Zhu, J., Baughman, J.M., Clayton, T., Slade, M., Wong, H.K., Danga, K., Zheng, X., Labow, M., LeBrun, L., et al. (2020). Cereblon Modulators Target ZBTB16 and Its Oncogenic Fusion Partners for Degradation via Distinct Structural Degrons. ACS Chem. Biol. *15*, 3149–3158. 10.1021/acschembio.0c00674.

37. Hansen, J.D., Correa, M., Nagy, M.A., Alexander, M., Plantevin, V., Grant, V., Whitefield, B., Huang, D., Kercher, T., Harris, R., et al. (2020). Discovery of CRBN E3 Ligase Modulator CC-92480 for the Treatment of Relapsed and Refractory Multiple Myeloma. J. Med. Chem. *63*, 6648–6676. 10.1021/acs.jmedchem.9b01928.

38. Powell, C.E., Du, G., Che, J., He, Z., Donovan, K.A., Yue, H., Wang, E.S., Nowak, R.P., Zhang, T., Fischer, E.S., et al. (2020). Selective Degradation of GSPT1 by Cereblon Modulators Identified via a Focused Combinatorial Library. ACS Chem. Biol. *15*, 2722–2730. 10.1021/acschembio.0c00520.

39. Surka, C., Jin, L., Mbong, N., Lu, C.-C., Jang, I.S., Rychak, E., Mendy, D., Clayton, T., Tindall, E., Hsu, C., et al. (2021). CC-90009, a novel cereblon E3 ligase modulator, targets acute myeloid leukemia blasts and leukemia stem cells. Blood *137*, 661–677. 10.1182/blood.2020008676.

40. Watson, E.R., Novick, S., Matyskiela, M.E., Chamberlain, P.P., H. De La Peña, A., Zhu, J., Tran, E., Griffin, P.R., Wertz, I.E., and Lander, G.C. (2022). Molecular glue CELMoD compounds are regulators of cereblon conformation. Science *378*, 549–553. 10.1126/science.add7574.

41. Han, T., Goralski, M., Gaskill, N., Capota, E., Kim, J., Ting, T.C., Xie, Y., Williams, N.S., and Nijhawan, D. (2017). Anticancer sulfonamides target splicing by inducing RBM39 degradation via recruitment to DCAF15. Science *356*, eaal3755. 10.1126/science.aal3755.

42. Uehara, T., Minoshima, Y., Sagane, K., Sugi, N.H., Mitsuhashi, K.O., Yamamoto, N., Kamiyama, H., Takahashi, K., Kotake, Y., Uesugi, M., et al. (2017). Selective degradation of splicing factor CAPERα by anticancer sulfonamides. Nat Chem Biol *13*, 675–680. 10.1038/nchembio.2363.

43. Du, X., Volkov, O.A., Czerwinski, R.M., Tan, H., Huerta, C., Morton, E.R., Rizzi, J.P., Wehn, P.M., Xu, R., Nijhawan, D., et al. (2019). Structural Basis and Kinetic Pathway of RBM39 Recruitment to DCAF15 by a Sulfonamide Molecular Glue E7820. Structure *27*, 1625-1633.e3. 10.1016/j.str.2019.10.005.

44. Bussiere, D.E., Xie, L., Srinivas, H., Shu, W., Burke, A., Be, C., Zhao, J., Godbole, A., King, D., Karki, R.G., et al. (2020). Structural basis of indisulam-mediated RBM39 recruitment to DCAF15 E3 ligase complex. Nat Chem Biol *16*, 15–23. 10.1038/s41589-019-0411-6.

45. Faust, T.B., Yoon, H., Nowak, R.P., Donovan, K.A., Li, Z., Cai, Q., Eleuteri, N.A., Zhang, T., Gray, N.S., and Fischer, E.S. (2020). Structural complementarity facilitates E7820-mediated degradation of RBM39 by DCAF15. Nat Chem Biol *16*, 7–14. 10.1038/s41589-019-0378-3.

46. Mayor-Ruiz, C., Bauer, S., Brand, M., Kozicka, Z., Siklos, M., Imrichova, H., Kaltheuner, I.H., Hahn, E., Seiler, K., Koren, A., et al. (2020). Rational discovery of molecular glue degraders via scalable chemical profiling. Nat Chem Biol *16*, 1199–1207. 10.1038/s41589-020-0594-x.

47. Słabicki, M., Kozicka, Z., Petzold, G., Li, Y.-D., Manojkumar, M., Bunker, R.D., Donovan, K.A., Sievers, Q.L., Koeppel, J., Suchyta, D., et al. (2020). The CDK inhibitor CR8 acts as a molecular glue degrader that depletes cyclin K. Nature *585*, 293–297. 10.1038/s41586-020-2374-x.

48. Lv, L., Chen, P., Cao, L., Li, Y., Zeng, Z., Cui, Y., Wu, Q., Li, J., Wang, J.-H., Dong, M.-Q., et al. (2020). Discovery of a molecular glue promoting CDK12-DDB1 interaction to trigger cyclin K degradation. eLife *9*, e59994. 10.7554/eLife.59994.

49. Dieter, S.M., Siegl, C., Codó, P.L., Huerta, M., Ostermann-Parucha, A.L., Schulz, E., Zowada, M.K., Martin, S., Laaber, K., Nowrouzi, A., et al. (2021). Degradation of CCNK/CDK12 is a druggable vulnerability of colorectal cancer. Cell Reports *36*, 109394. 10.1016/j.celrep.2021.109394.

50. Jorda, R., Havlíček, L., Peřina, M., Vojáčková, V., Pospíšil, T., Djukic, S., Škerlová, J., Grúz, J., Renešová, N., Klener, P., et al. (2022). 3,5,7-Substituted Pyrazolo[4,3- *d*]Pyrimidine Inhibitors of Cyclin-Dependent Kinases and Cyclin K Degraders. J. Med. Chem. *65*, 8881–8896. 10.1021/acs.jmedchem.1c02184.

51. Kozicka, Z., Suchyta, D.J., Focht, V., Kempf, G., Petzold, G., Jentzsch, M., Zou, C., Di Genua, C., Donovan, K.A., Coomar, S., et al. (2023). Design principles for cyclin K molecular glue degraders. Nat Chem Biol. 10.1038/s41589-023-01409-z.

52. Simonetta, K.R., Taygerly, J., Boyle, K., Basham, S.E., Padovani, C., Lou, Y., Cummins, T.J., Yung, S.L., Von Soly, S.K., Kayser, F., et al. (2019). Prospective discovery of small molecule enhancers of an E3 ligase-substrate interaction. Nat Commun *10*, 1402. 10.1038/s41467-019-09358-9.

53. Huai, Q., Kim, H.-Y., Liu, Y., Zhao, Y., Mondragon, A., Liu, J.O., and Ke, H. (2002). Crystal structure of calcineurin–cyclophilin–cyclosporin shows common but distinct recognition of immunophilin–drug complexes. Proc. Natl. Acad. Sci. U.S.A. *99*, 12037–12042. 10.1073/pnas.192206699.

54. Griffith, J.P., Kim, J.L., Kim, E.E., Sintchak, M.D., Thomson, J.A., Fitzgibbon, M.J., Fleming, M.A., Caron, P.R., Hsiao, K., and Navia, M.A. (1995). X-ray structure of calcineurin inhibited by the immunophilin-immunosuppressant FKBP12-FK506 complex. Cell *82*, 507–522. 10.1016/0092-8674(95)90439-5.

55. Choi, J., Chen, J., Schreiber, S.L., and Clardy, J. (1996). Structure of the FKBP12-Rapamycin Complex Interacting with Binding Domain of Human FRAP. Science *273*, 239–242. 10.1126/science.273.5272.239.

56. De Vries-van Leeuwen, I.J., da Costa Pereira, D., Flach, K.D., Piersma, S.R., Haase, C., Bier, D., Yalcin, Z., Michalides, R., Feenstra, K.A., Jiménez, C.R., et al. (2013). Interaction of 14-3-3 proteins with the estrogen receptor alpha F domain provides a drug target interface. Proc Natl Acad Sci U S A *110*, 8894–8899. 10.1073/pnas.1220809110.

57. De Vink, P.J., Andrei, S.A., Higuchi, Y., Ottmann, C., Milroy, L.-G., and Brunsveld, L. (2019). Cooperativity basis for small-molecule stabilization of protein–protein interactions. Chem. Sci. *10*, 2869–2874. 10.1039/C8SC05242E.

58. Brink, H.J., Van Senten, J.R., De Vries-van Leeuwen, I.J., Da Costa Pereira, D., Piersma, S.R., Jimenez, C.R., Centorrino, F., Ottmann, C., Siderius, M., Smit, M.J., et al. (2022). Fusicoccin-A Targets Cancerous Inhibitor of Protein Phosphatase 2A by Stabilizing a C-Terminal Interaction with 14-3-3. ACS Chem. Biol. *17*, 2972–2978. 10.1021/acschembio.2c00299.

59. Molzan, M., Kasper, S., Röglin, L., Skwarczynska, M., Sassa, T., Inoue, T., Breitenbuecher, F., Ohkanda, J., Kato, N., Schuler, M., et al. (2013). Stabilization of physical RAF/14-3-3 interaction by cotylenin A as treatment strategy for RAS mutant cancers. ACS Chem Biol *8*, 1869–1875. 10.1021/cb4003464.

60. Aitken, A. (2006). 14-3-3 proteins: a historic overview. Semin Cancer Biol *16*, 162–172. 10.1016/j.semcancer.2006.03.005.

61. Sluchanko, N.N. (2020). Reading the phosphorylation code: binding of the 14-3-3 protein to multivalent client phosphoproteins. Biochemical Journal *477*, 1219–1225. 10.1042/BCJ20200084.

62. Sato, S., Jung, H., Nakagawa, T., Pawlosky, R., Takeshima, T., Lee, W.-R., Sakiyama, H., Laxman, S., Wynn, R.M., Tu, B.P., et al. (2016). Metabolite Regulation of Nuclear Localization of Carbohydrate-

response Element-binding Protein (ChREBP). Journal of Biological Chemistry *291*, 10515–10527. 10.1074/jbc.M115.708982.

63. Kondo, Y., Ognjenović, J., Banerjee, S., Karandur, D., Merk, A., Kulhanek, K., Wong, K., Roose, J.P., Subramaniam, S., and Kuriyan, J. (2019). Cryo-EM structure of a dimeric B-Raf:14-3-3 complex reveals asymmetry in the active sites of B-Raf kinases. Science *366*, 109–115. 10.1126/science.aay0543.

64. Okamoto, K., and Sako, Y. (2023). Two Closed Conformations of CRAF Require the 14-3-3 Binding Motifs and Cysteine-Rich Domain to be Intact in Live Cells. Journal of Molecular Biology *435*, 167989. 10.1016/j.jmb.2023.167989.

65. Park, E., Rawson, S., Li, K., Kim, B.-W., Ficarro, S.B., Pino, G.G.-D., Sharif, H., Marto, J.A., Jeon, H., and Eck, M.J. (2019). Architecture of autoinhibited and active BRAF-MEK1-14-3-3 complexes. Nature *575*, 545–550. 10.1038/s41586-019-1660-y.

66. Martinez Fiesco, J.A., Durrant, D.E., Morrison, D.K., and Zhang, P. (2022). Structural insights into the BRAF monomer-to-dimer transition mediated by RAS binding. Nat Commun *13*, 486. 10.1038/s41467-022-28084-3.

67. García-Alonso, S., Mesa, P., De La Puente Ovejero, L., Aizpurua, G., Lechuga, C.G., Zarzuela, E., Santiveri, C.M., Sanclemente, M., Muñoz, J., Musteanu, M., et al. (2022). Structure of the RAF1-HSP90-CDC37 complex reveals the basis of RAF1 regulation (Biochemistry) 10.1101/2022.05.04.490607.

68. Sijbesma, E., Visser, E., Plitzko, K., Thiel, P., Milroy, L.-G., Kaiser, M., Brunsveld, L., and Ottmann, C. (2020). Structure-based evolution of a promiscuous inhibitor to a selective stabilizer of protein–protein interactions. Nat Commun *11*, 3954. 10.1038/s41467-020-17741-0.

69. Soini, L., Redhead, M., Westwood, M., Leysen, S., Davis, J., and Ottmann, C. (2021). Identification of molecular glues of the SLP76/14-3-3 protein–protein interaction. RSC Med. Chem. *12*, 1555–1564. 10.1039/D1MD00172H.

70. Rose, R., Erdmann, S., Bovens, S., Wolf, A., Rose, M., Hennig, S., Waldmann, H., and Ottmann, C. (2010). Identification and Structure of Small-Molecule Stabilizers of 14 – 3 – 3 Protein–Protein Interactions. Angew Chem Int Ed *49*, 4129–4132. 10.1002/anie.200907203.

71. Guillory, X., Wolter, M., Leysen, S., Neves, J.F., Kuusk, A., Genet, S., Somsen, B., Morrow, J.K., Rivers, E., van Beek, L., et al. (2020). Fragment-based Differential Targeting of PPI Stabilizer Interfaces. J Med Chem *63*, 6694–6707. 10.1021/acs.jmedchem.9b01942.

72. Sijbesma, E., Hallenbeck, K.K., Leysen, S., de Vink, P.J., Skóra, L., Jahnke, W., Brunsveld, L., Arkin, M.R., and Ottmann, C. (2019). Site-Directed Fragment-Based Screening for the Discovery of Protein-Protein Interaction Stabilizers. J Am Chem Soc *141*, 3524–3531. 10.1021/jacs.8b11658.

73. Wolter, M., Valenti, D., Cossar, P.J., Levy, L.M., Hristeva, S., Genski, T., Hoffmann, T., Brunsveld, L., Tzalis, D., and Ottmann, C. (2020). Fragment-Based Stabilizers of Protein-Protein Interactions through Imine-Based Tethering. Angew Chem Int Ed Engl *59*, 21520–21524. 10.1002/anie.202008585.

74. Kenanova, D.N., Visser, E.J., Virta, J.M., Sijbesma, E., Centorrino, F., Vickery, H.R., Zhong, M., Neitz, R.J., Brunsveld, L., Ottmann, C., et al. (2023). A Systematic Approach to the Discovery of Protein–Protein Interaction Stabilizers. ACS Cent. Sci. *9*, 937–946. 10.1021/acscentsci.2c01449.

75. Sijbesma, E., Somsen, B.A., Miley, G.P., Leijten-van de Gevel, I.A., Brunsveld, L., Arkin, M.R., and Ottmann, C. (2020). Fluorescence Anisotropy-Based Tethering for Discovery of Protein-Protein Interaction Stabilizers. ACS Chem Biol *15*, 3143–3148. 10.1021/acschembio.0c00646.

76. Ge, Q., Huang, N., Wynn, R.M., Li, Y., Du, X., Miller, B., Zhang, H., and Uyeda, K. (2012). Structural Characterization of a Unique Interface between Carbohydrate Response Element-binding Protein (ChREBP) and 14-3-3β Protein. Journal of Biological Chemistry *287*, 41914–41921. 10.1074/jbc.M112.418855.

77. Visser, E.J. (2023). Evolution of 14-3-3 molecular glues: from fragment hits to cellularly active leads, 2023, ISBN 978-90-386-5759-2 (Gildeprint).

78. Fuller, J.C., Burgoyne, N.J., and Jackson, R.M. (2009). Predicting druggable binding sites at the protein–protein interface. Drug Discovery Today *14*, 155–161. 10.1016/j.drudis.2008.10.009.

79. Cossar, P.J., Wolter, M., van Dijck, L., Valenti, D., Levy, L.M., Ottmann, C., and Brunsveld, L. (2021). Reversible Covalent Imine-Tethering for Selective Stabilization of 14-3-3 Hub Protein Interactions. J Am Chem Soc *143*, 8454–8464. 10.1021/jacs.1c03035.

80. Hallenbeck, K.K., Davies, J.L., Merron, C., Ogden, P., Sijbesma, E., Ottmann, C., Renslo, A.R., Wilson, C., and Arkin, M.R. (2017). A Liquid Chromatography/Mass Spectrometry Method for Screening Disulfide Tethering Fragments. SLAS Discov, 2472555217732072. 10.1177/2472555217732072.

81. Visser, E.J., Jaishankar, P., Sijbesma, E., Pennings, M.A.M., Vandenboorn, E.M.F., Guillory, X., Neitz, R.J., Morrow, J., Dutta, S., Renslo, A.R., et al. (2023). From Tethered to Freestanding Stabilizers of 14-3-3 Protein-Protein Interactions through Fragment Linking. Angew Chem Int Ed *62*, e202308004. 10.1002/anie.202308004.

82. Konstantinidou, M., Visser, E.J., Vandenboorn, E., Chen, S., Jaishankar, P., Overmans, M., Dutta, S., Neitz, R.J., Renslo, A.R., Ottmann, C., et al. (2023). Structure-Based Optimization of Covalent, Small-Molecule Stabilizers of the 14-3-3σ/ERα Protein–Protein Interaction from Nonselective Fragments. J. Am. Chem. Soc. *145*, 20328–20343. 10.1021/jacs.3c05161.

83. Khan, Z.M., Real, A.M., Marsiglia, W.M., Chow, A., Duffy, M.E., Yerabolu, J.R., Scopton, A.P., and Dar, A.C. (2020). Structural basis for the action of the drug trametinib at KSR-bound MEK. Nature *588*, 509–514. 10.1038/s41586-020-2760-4.

84. Bueno, A.B., Sun, B., Willard, F.S., Feng, D., Ho, J.D., Wainscott, D.B., Showalter, A.D., Vieth, M., Chen, Q., Stutsman, C., et al. (2020). Structural insights into probe-dependent positive allosterism of the GLP-1 receptor. Nat Chem Biol *16*, 1105–1110. 10.1038/s41589-020-0589-7.

85. Johnson, S.M., Connelly, S., Fearns, C., Powers, E.T., and Kelly, J.W. (2012). The Transthyretin Amyloidoses: From Delineating the Molecular Mechanism of Aggregation Linked to Pathology to a

Regulatory-Agency-Approved Drug. Journal of Molecular Biology *421*, 185–203. 10.1016/j.jmb.2011.12.060.

86. Kerres, N., Steurer, S., Schlager, S., Bader, G., Berger, H., Caligiuri, M., Dank, C., Engen, J.R., Ettmayer, P., Fischerauer, B., et al. (2017). Chemically Induced Degradation of the Oncogenic Transcription Factor BCL6. Cell Reports *20*, 2860–2875. 10.1016/j.celrep.2017.08.081.

87. Słabicki, M., Yoon, H., Koeppel, J., Nitsch, L., Roy Burman, S.S., Di Genua, C., Donovan, K.A., Sperling, A.S., Hunkeler, M., Tsai, J.M., et al. (2020). Small-molecule-induced polymerization triggers degradation of BCL6. Nature *588*, 164–168. 10.1038/s41586-020-2925-1.

88. Bellenie, B.R., Cheung, K.-M.J., Varela, A., Pierrat, O.A., Collie, G.W., Box, G.M., Bright, M.D., Gowan, S., Hayes, A., Rodrigues, M.J., et al. (2020). Achieving *In Vivo* Target Depletion through the Discovery and Optimization of Benzimidazolone BCL6 Degraders. J. Med. Chem. *63*, 4047–4068. 10.1021/acs.jmedchem.9b02076.

89. Sun, C., Mezzadra, R., and Schumacher, T.N. (2018). Regulation and Function of the PD-L1 Checkpoint. Immunity *48*, 434–452. 10.1016/j.immuni.2018.03.014.

90. Ghosh, C., Luong, G., and Sun, Y. (2021). A snapshot of the PD-1/PD-L1 pathway. J. Cancer *12*, 2735–2746. 10.7150/jca.57334.

91. Ai, L., Xu, A., and Xu, J. (2020). Roles of PD-1/PD-L1 Pathway: Signaling, Cancer, and Beyond. In Regulation of Cancer Immune Checkpoints Advances in Experimental Medicine and Biology., J. Xu, ed. (Springer Singapore), pp. 33–59. 10.1007/978-981-15-3266-5_3.

92. Zarganes-Tzitzikas, T., Konstantinidou, M., Gao, Y., Krzemien, D., Zak, K., Dubin, G., Holak, T.A., and Dömling, A. (2016). Inhibitors of programmed cell death 1 (PD-1): a patent review (2010-2015). Expert Opinion on Therapeutic Patents *26*, 973–977. 10.1080/13543776.2016.1206527.

93. Shaabani, S., Huizinga, H.P.S., Butera, R., Kouchi, A., Guzik, K., Magiera-Mularz, K., Holak, T.A., and Dömling, A. (2018). A patent review on PD-1/PD-L1 antagonists: small molecules, peptides, and macrocycles (2015-2018). Expert Opinion on Therapeutic Patents *28*, 665–678. 10.1080/13543776.2018.1512706.

94. Deng, J., Cheng, Z., Long, J., Dömling, A., Tortorella, M., and Wang, Y. (2022). Small Molecule Inhibitors of Programmed Cell Death Ligand 1 (PD-L1): A Patent Review (2019–2021). Expert Opinion on Therapeutic Patents *32*, 575–589. 10.1080/13543776.2022.2045276.

95. Abdel-Magid, A.F. (2015). Inhibitors of the PD-1/PD-L1 Pathway Can Mobilize the Immune System: An Innovative Potential Therapy for Cancer and Chronic Infections. ACS Med. Chem. Lett. *6*, 489–490. 10.1021/acsmedchemlett.5b00148.

96. Chupak, L.S., Zheng X. Compounds useful as immunomodulators, Briston-Myers Squibb, WO2015034820A1 (2015).

97. Zak, K.M., Grudnik, P., Guzik, K., Zieba, B.J., Musielak, B., Dömling, A., Dubin, G., and Holak, T.A. (2016). Structural basis for small molecule targeting of the programmed death ligand 1 (PD-L1). Oncotarget *7*, 30323–30335. 10.18632/oncotarget.8730.

98. Skalniak, L., Zak, K.M., Guzik, K., Magiera, K., Musielak, B., Pachota, M., Szelazek, B., Kocik, J., Grudnik, P., Tomala, M., et al. (2017). Small-molecule inhibitors of PD-1/PD-L1 immune checkpoint alleviate the PD-L1-induced exhaustion of T-cells. Oncotarget *8*, 72167–72181. 10.18632/oncotarget.20050.

99. Qin, M., Cao, Q., Zheng, S., Tian, Y., Zhang, H., Xie, J., Xie, H., Liu, Y., Zhao, Y., and Gong, P. (2019). Discovery of [1,2,4]Triazolo[4,3- *a*]pyridines as Potent Inhibitors Targeting the Programmed Cell Death-1/Programmed Cell Death-Ligand 1 Interaction. J. Med. Chem. *62*, 4703–4715. 10.1021/acs.jmedchem.9b00312.

100. Muszak, D., Surmiak, E., Plewka, J., Magiera-Mularz, K., Kocik-Krol, J., Musielak, B., Sala, D., Kitel, R., Stec, M., Weglarczyk, K., et al. (2021). Terphenyl-Based Small-Molecule Inhibitors of Programmed Cell Death-1/Programmed Death-Ligand 1 Protein–Protein Interaction. J. Med. Chem. *64*, 11614–11636. 10.1021/acs.jmedchem.1c00957.

101. Liu, L., Yao, Z., Wang, S., Xie, T., Wu, G., Zhang, H., Zhang, P., Wu, Y., Yuan, H., and Sun, H. (2021). Syntheses, Biological Evaluations, and Mechanistic Studies of Benzo[*c*][1,2,5]oxadiazole Derivatives as Potent PD-L1 Inhibitors with *In Vivo* Antitumor Activity. J. Med. Chem. *64*, 8391–8409. 10.1021/acs.jmedchem.1c00392.

102. OuYang, Y., Gao, J., Zhao, L., Lu, J., Zhong, H., Tang, H., Jin, S., Yue, L., Li, Y., Guo, W., et al. (2021). Design, Synthesis, and Evaluation of *o* -(Biphenyl-3-ylmethoxy)nitrophenyl Derivatives as PD-1/PD-L1 Inhibitors with Potent Anticancer Efficacy *In Vivo*. J. Med. Chem. *64*, 7646–7666. 10.1021/acs.jmedchem.1c00370.

103. Wang, T., Cai, S., Wang, M., Zhang, W., Zhang, K., Chen, D., Li, Z., and Jiang, S. (2021). Novel Biphenyl Pyridines as Potent Small-Molecule Inhibitors Targeting the Programmed Cell Death-1/Programmed Cell Death-Ligand 1 Interaction. J. Med. Chem. *64*, 7390–7403. 10.1021/acs.jmedchem.1c00010.

104. Song, Z., Liu, B., Peng, X., Gu, W., Sun, Y., Xing, L., Xu, Y., Geng, M., Ai, J., and Zhang, A. (2021). Design, Synthesis, and Pharmacological Evaluation of Biaryl-Containing PD-1/PD-L1 Interaction Inhibitors Bearing a Unique Difluoromethyleneoxy Linkage. J. Med. Chem. *64*, 16687–16702. 10.1021/acs.jmedchem.1c01422.

105. Butera, R., Ważyńska, M., Magiera-Mularz, K., Plewka, J., Musielak, B., Surmiak, E., Sala, D., Kitel, R., De Bruyn, M., Nijman, H.W., et al. (2021). Design, Synthesis, and Biological Evaluation of Imidazopyridines as PD-1/PD-L1 Antagonists. ACS Med. Chem. Lett. *12*, 768–773. 10.1021/acsmedchemlett.1c00033.

106. Chen, F.-F., Li, Z., Ma, D., and Yu, Q. (2020). Small-molecule PD-L1 inhibitor BMS1166 abrogates the function of PD-L1 by blocking its ER export. OncoImmunology *9*, 1831153. 10.1080/2162402X.2020.1831153.

107. Wang, T., Cai, S., Cheng, Y., Zhang, W., Wang, M., Sun, H., Guo, B., Li, Z., Xiao, Y., and Jiang, S. (2022). Discovery of Small-Molecule Inhibitors of the PD-1/PD-L1 Axis That Promote PD-L1 Internalization and Degradation. J. Med. Chem. *65*, 3879–3893. 10.1021/acs.jmedchem.1c01682.

108. Wojtaszek, J.L., Chatterjee, N., Najeeb, J., Ramos, A., Lee, M., Bian, K., Xue, J.Y., Fenton, B.A., Park, H., Li, D., et al. (2019). A Small Molecule Targeting Mutagenic Translesion Synthesis Improves Chemotherapy. Cell *178*, 152-159.e11. 10.1016/j.cell.2019.05.028.

109. Li, J., Canham, S.M., Wu, H., Henault, M., Chen, L., Liu, G., Chen, Y., Yu, G., Miller, H.R., Hornak, V., et al. (2023). Activation of human STING by a molecular glue-like compound. Nat Chem Biol. 10.1038/s41589-023-01434-y.

110. Lu, D., Shang, G., Li, J., Lu, Y., Bai, X., and Zhang, X. (2022). Activation of STING by targeting a pocket in the transmembrane domain. Nature *604*, 557–562. 10.1038/s41586-022-04559-7.

111. Lin, S.-M., Lin, S.-C., Hsu, J.-N., Chang, C., Chien, C.-M., Wang, Y.-S., Wu, H.-Y., Jeng, U.-S., Kehn-Hall, K., and Hou, M.-H. (2020). Structure-Based Stabilization of Non-native Protein–Protein Interactions of Coronavirus Nucleocapsid Proteins in Antiviral Drug Design. J. Med. Chem. *63*, 3131–3141. 10.1021/acs.jmedchem.9b01913.

112. Sidrauski, C., Acosta-Alvear, D., Khoutorsky, A., Vedantham, P., Hearn, B.R., Li, H., Gamache, K., Gallagher, C.M., Ang, K.K.-H., Wilson, C., et al. (2013). Pharmacological brake-release of mRNA translation enhances cognitive memory. eLife *2*, e00498. 10.7554/eLife.00498.

113. Bogorad, A.M., Xia, B., Sandor, D.G., Mamonov, A.B., Cafarella, T.R., Jehle, S., Vajda, S., Kozakov, D., and Marintchev, A. (2014). Insights into the Architecture of the eIF2Bα/β/δ Regulatory Subcomplex. Biochemistry *53*, 3432–3445. 10.1021/bi500346u.

114. Wortham, N.C., and Proud, C.G. (2015). eIF2B: recent structural and functional insights into a key regulator of translation. Biochemical Society Transactions *43*, 1234–1240. 10.1042/BST20150164.

115. Sidrauski, C., Tsai, J.C., Kampmann, M., Hearn, B.R., Vedantham, P., Jaishankar, P., Sokabe, M., Mendez, A.S., Newton, B.W., Tang, E.L., et al. (2015). Pharmacological dimerization and activation of the exchange factor eIF2B antagonizes the integrated stress response. eLife *4*, e07314. 10.7554/eLife.07314.

116. Sekine, Y., Zyryanova, A., Crespillo-Casado, A., Fischer, P.M., Harding, H.P., and Ron, D. (2015). Mutations in a translation initiation factor identify the target of a memory-enhancing compound. Science *348*, 1027–1030. 10.1126/science.aaa6986.

117. Hearn, B.R., Jaishankar, P., Sidrauski, C., Tsai, J.C., Vedantham, P., Fontaine, S.D., Walter, P., and Renslo, A.R. (2016). Structure–Activity Studies of Bis- *O* -Arylglycolamides: Inhibitors of the Integrated Stress Response. ChemMedChem *11*, 870–880. 10.1002/cmdc.201500483.

118. Tsai, J.C., Miller-Vedam, L.E., Anand, A.A., Jaishankar, P., Nguyen, H.C., Renslo, A.R., Frost, A., and Walter, P. (2018). Structure of the nucleotide exchange factor eIF2B reveals mechanism of memory-enhancing molecule. Science *359*, eaaq0939. 10.1126/science.aaq0939.

119. Zyryanova, A.F., Kashiwagi, K., Rato, C., Harding, H.P., Crespillo-Casado, A., Perera, L.A., Sakamoto, A., Nishimoto, M., Yonemochi, M., Shirouzu, M., et al. (2021). ISRIB Blunts the Integrated Stress Response by Allosterically Antagonising the Inhibitory Effect of Phosphorylated eIF2 on eIF2B. Molecular Cell *81*, 88-103.e6. 10.1016/j.molcel.2020.10.031.

120. Schoof, M., Boone, M., Wang, L., Lawrence, R., Frost, A., and Walter, P. (2021). eIF2B conformation and assembly state regulate the integrated stress response. eLife *10*, e65703. 10.7554/eLife.65703.

121. Morreale, F.E., Testa, A., Chaugule, V.K., Bortoluzzi, A., Ciulli, A., and Walden, H. (2017). Mind the Metal: A Fragment Library-Derived Zinc Impurity Binds the E2 Ubiquitin-Conjugating Enzyme Ube2T and Induces Structural Rearrangements. J Med Chem *60*, 8183–8191. 10.1021/acs.jmedchem.7b01071.

122. Swinney, D.C. (2013). Phenotypic vs. Target-Based Drug Discovery for First-in-Class Medicines. Clin Pharmacol Ther *93*, 299–301. 10.1038/clpt.2012.236.

123. Luo, M., Spradlin, J.N., Boike, L., Tong, B., Brittain, S.M., McKenna, J.M., Tallarico, J.A., Schirle, M., Maimone, T.J., and Nomura, D.K. (2021). Chemoproteomics-enabled discovery of covalent RNF114-based degraders that mimic natural product function. Cell Chemical Biology *28*, 559-566.e15. 10.1016/j.chembiol.2021.01.005.

124. King, E.A., Cho, Y., Hsu, N.S., Dovala, D., McKenna, J.M., Tallarico, J.A., Schirle, M., and Nomura, D.K. (2023). Chemoproteomics-enabled discovery of a covalent molecular glue degrader targeting NF-κB. Cell Chemical Biology *30*, 394-402.e9. 10.1016/j.chembiol.2023.02.008.

125. Kong, N.R., and Jones, L.H. (2023). Clinical Translation of Targeted Protein Degraders. Clin Pharma and Therapeutics *114*, 558–568. 10.1002/cpt.2985.

126. Sasso, J.M., Tenchov, R., Wang, D., Johnson, L.S., Wang, X., and Zhou, Q.A. (2023). Molecular Glues: The Adhesive Connecting Targeted Protein Degradation to the Clinic. Biochemistry *62*, 601–623. 10.1021/acs.biochem.2c00245.

127. Cao, S., Kang, S., Mao, H., Yao, J., Gu, L., and Zheng, N. (2022). Defining molecular glues with a dual-nanobody cannabidiol sensor. Nat Commun *13*, 815. 10.1038/s41467-022-28507-1.

128. Hsia, O., Hinterndorfer, M., Cowan, A.D., Iso, K., Ishida, T., Sundaramoorthy, R., Nakasone, M.A., Imrichova, H., Schätz, C., Rukavina, A., et al. (2024). Targeted protein degradation via intramolecular bivalent glues. Nature. 10.1038/s41586-024-07089-6.

129. Hanan, E.J., Braun, M.-G., Heald, R.A., MacLeod, C., Chan, C., Clausen, S., Edgar, K.A., Eigenbrot, C., Elliott, R., Endres, N., et al. (2022). Discovery of GDC-0077 (Inavolisib), a Highly Selective Inhibitor and Degrader of Mutant PI3Kα. J. Med. Chem. *65*, 16589–16621. 10.1021/acs.jmedchem.2c01422.

130. Blake, R.A. (2019). Abstract 4452: GNE-0011, a novel monovalent BRD4 degrader. Cancer Research *79*, 4452–4452. 10.1158/1538-7445.AM2019-4452.

131. Blake, R.A. et al Tert-butyl (s)-2-(4-(phenyl)-6h-thieno[3,2-f][1,2,4]triazolo[4,3-a] [1,4]diazepin-6-yl) acetate derivatives and related compounds as bromodomain BRD4inhibitors for treating cancer. Genentech, International Patent No. PCT/US2019/050576 (WO/2020/055976) (2020).

132. Shergalis, A.G., Marin, V.L., Rhee, D.Y., Senaweera, S., McCloud, R.L., Ronau, J.A., Hutchins, C.W., McLoughlin, S., Woller, K.R., Warder, S.E., et al. (2023). CRISPR Screen Reveals BRD2/4 Molecular

Glue-like Degrader via Recruitment of DCAF16. ACS Chem. Biol. *18*, 331–339. 10.1021/acschembio.2c00747.

133. Li, Y.-D., Ma, M.W., Hassan, M.M., Hunkeler, M., Teng, M., Puvar, K., Lumpkin, R., Sandoval, B., Jin, C.Y., Ficarro, S.B., et al. (2023). Template-assisted covalent modification of DCAF16 underlies activity of BRD4 molecular glue degraders (Biochemistry) 10.1101/2023.02.14.528208.

134. Schulze, C.J., Seamon, K.J., Zhao, Y., Yang, Y.C., Cregg, J., Kim, D., Tomlinson, A., Choy, T.J., Wang, Z., Sang, B., et al. (2023). Chemical remodeling of a cellular chaperone to target the active state of mutant KRAS. Science *381*, 794–799. 10.1126/science.adg9652.

Figure 1

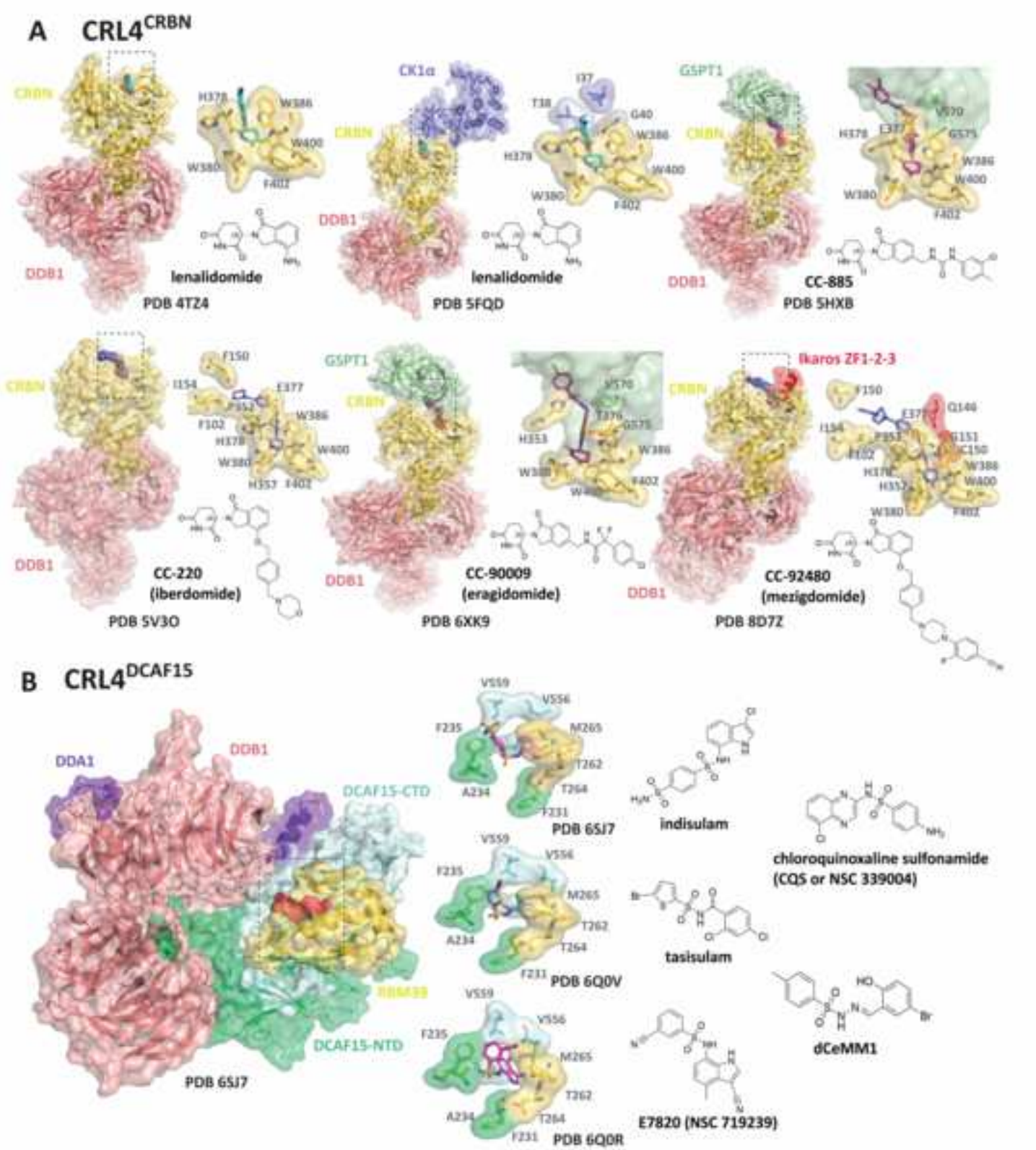

Figure 2

Click here to access/download;Figure;Fig2.tif

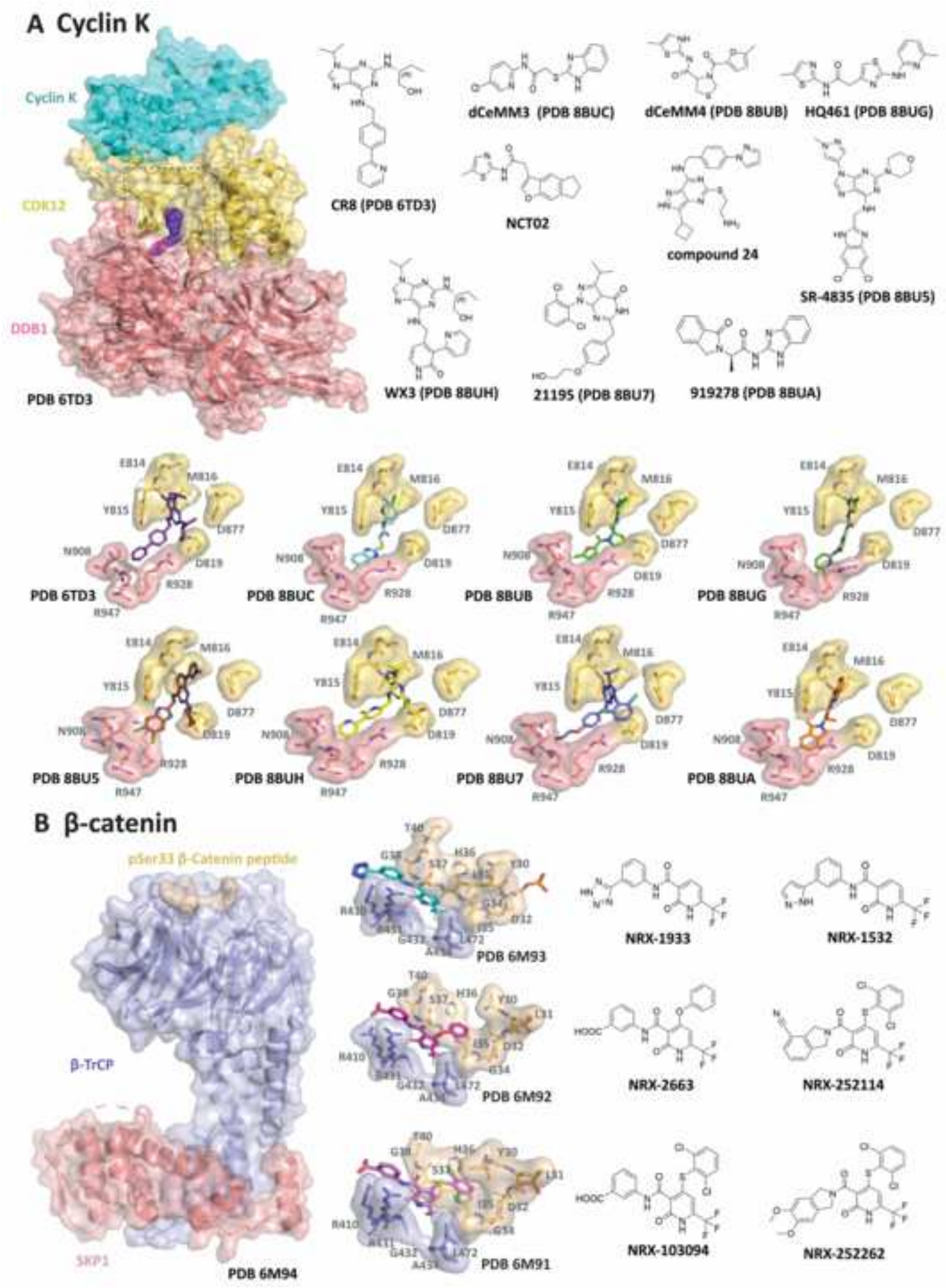

Figure 3

Click here to access/download;Figure;Fig3.tif

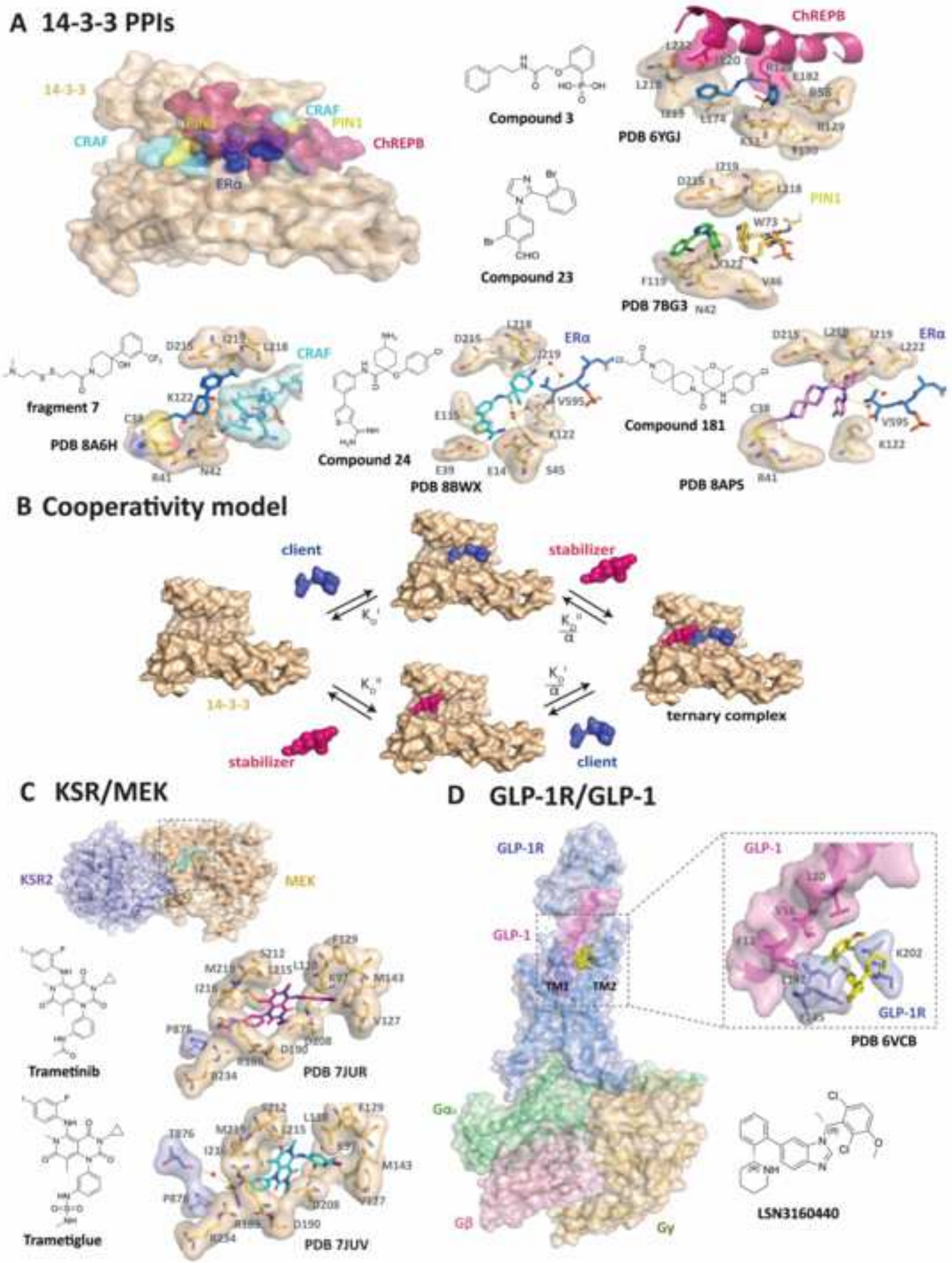

Figure 4

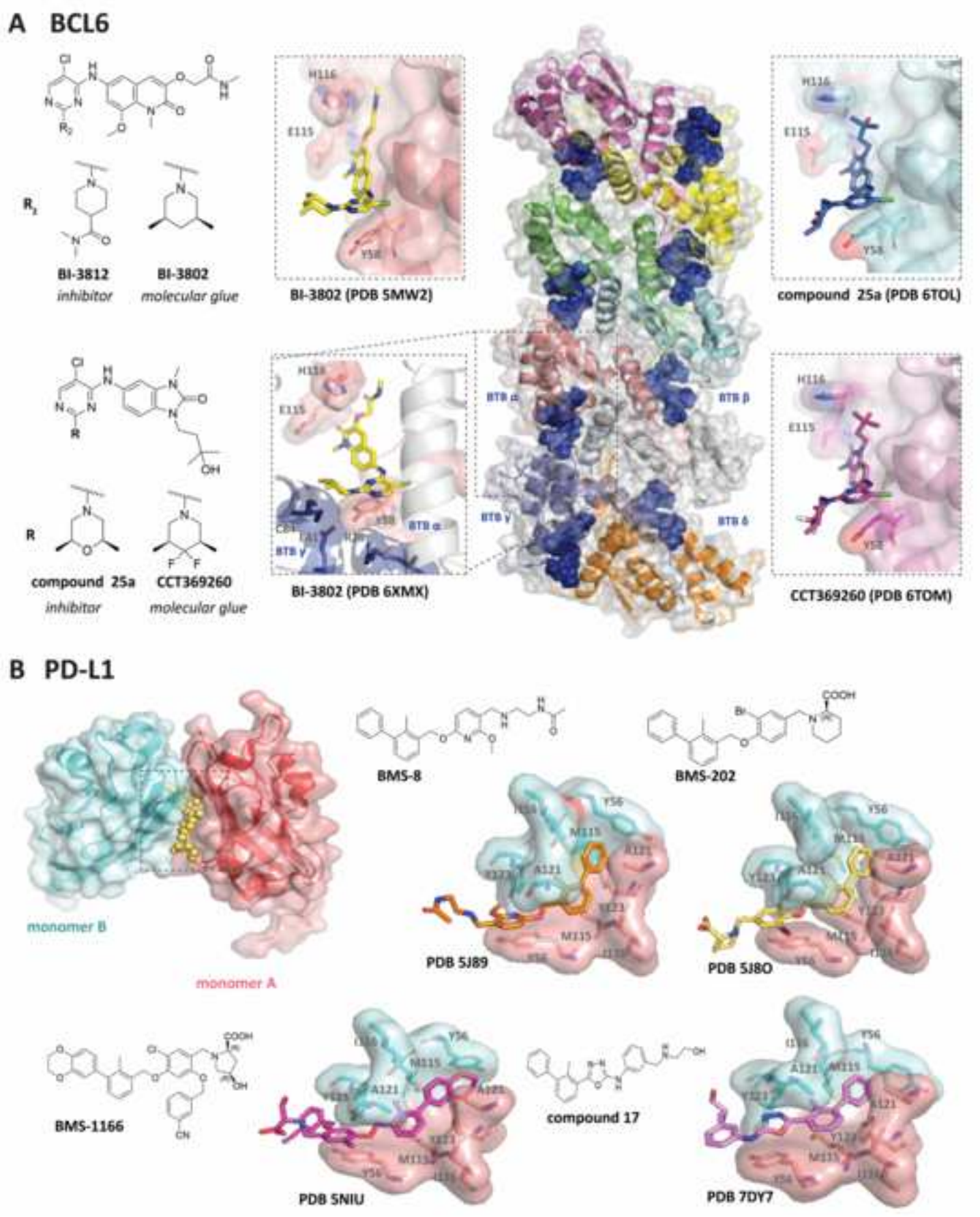

Figure 5

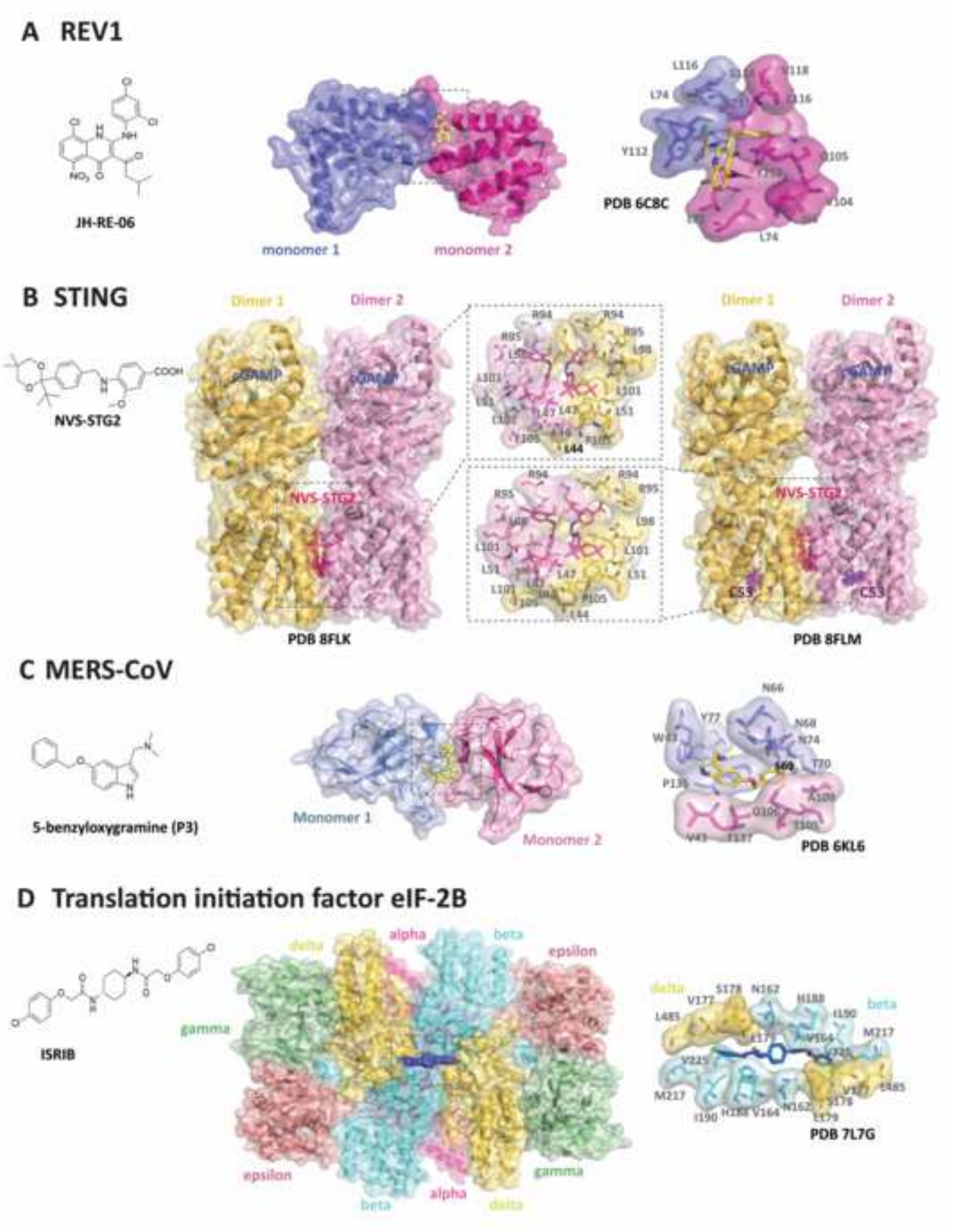

Figure 6

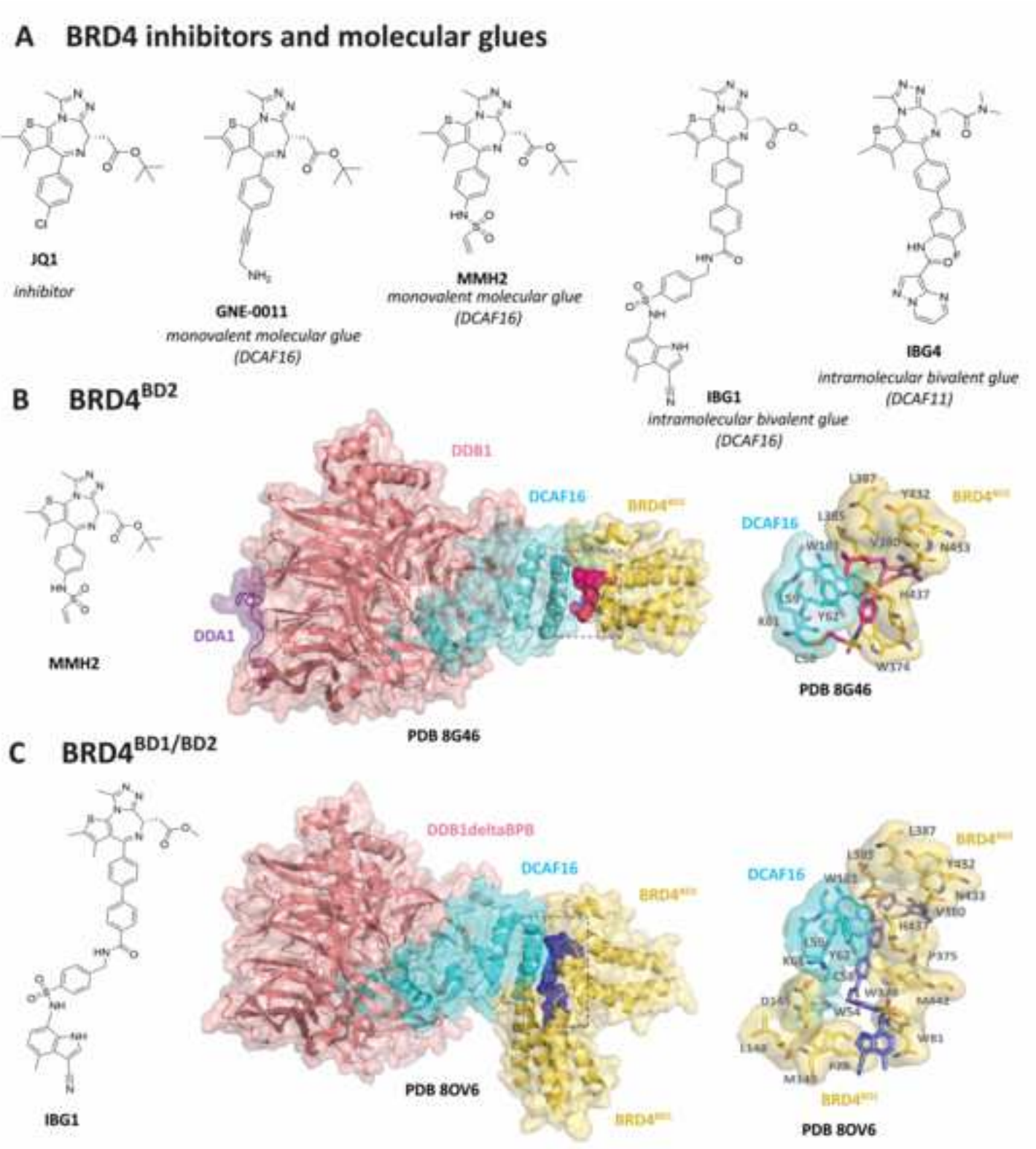

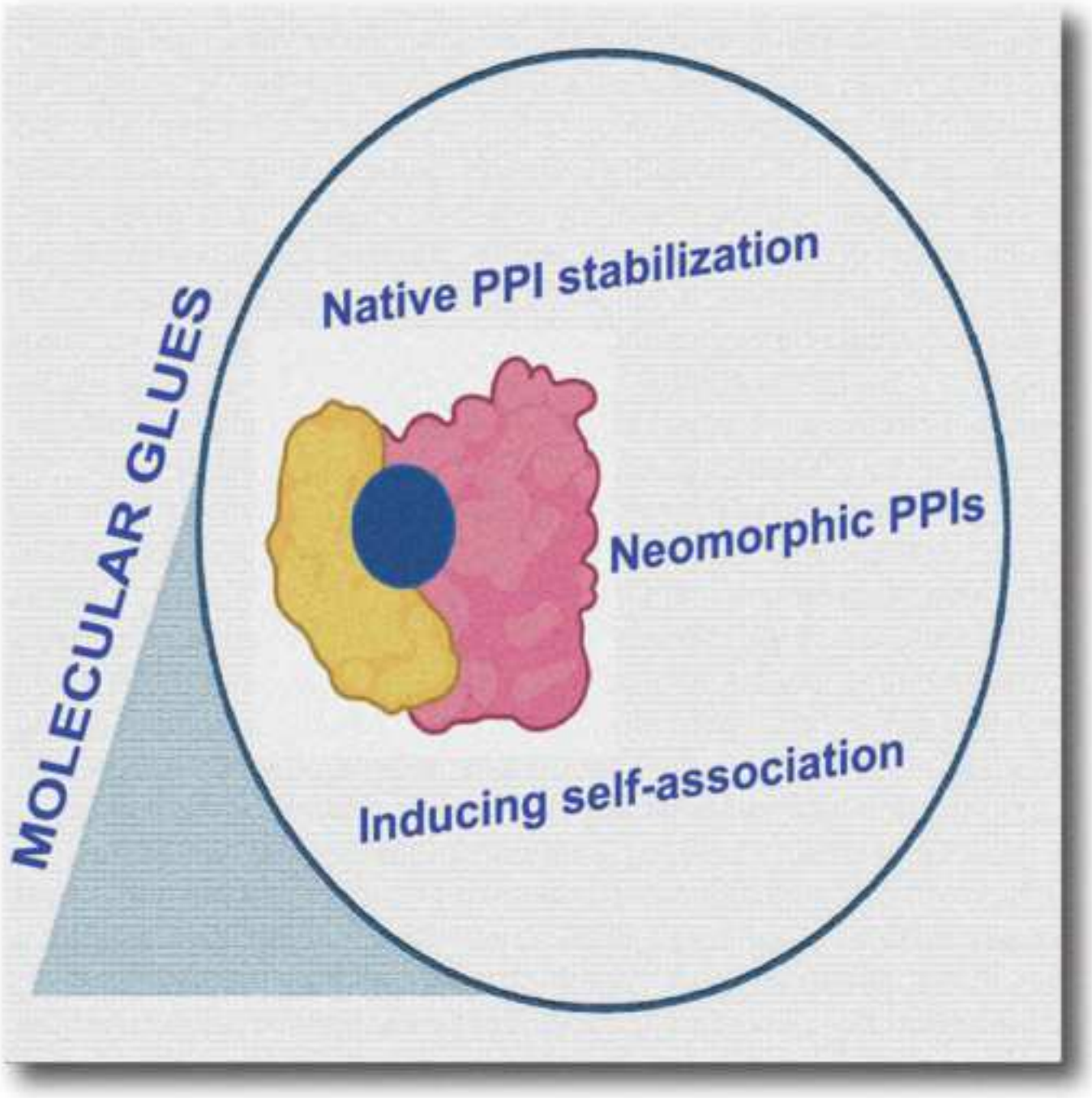

Table S1

Click here to access/download

Supplemental Videos and Spreadsheets

Table S1.xlsx